

Development and analysis of an *in vitro* model of
inflammatory cytokine-mediated idiosyncratic drug hepatotoxicity

by

Maya Hasan

B.S. Biology

Massachusetts Institute of Technology, 2006

Submitted to the Department of Biological Engineering in
Partial Fulfillment of the Requirements for the Degree of

Master of Engineering in Biomedical Engineering
at the
Massachusetts Institute of Technology

September 2007

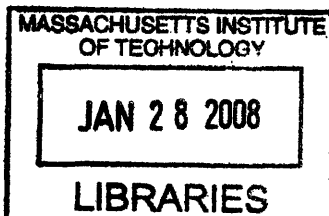
© 2007 Massachusetts Institute of Technology.
All Rights Reserved.

Signature of Author: _____
Department of Biological Engineering
August 10, 2007

Certified by: _____
Douglas A. Lauffenburger
Whitaker Professor of Bioengineering, Chemical Engineering, and Biology
Director, Biological Engineering Division
Thesis Supervisor

Accepted by: _____
Bevin P. Engelward
Associate Professor of Biological Engineering
MEBE Program Director

Accepted by: _____
Alan J. Grodzinsky
Professor of Electrical, Mechanical, and Biological Engineering
Director, Center for Biomedical Engineering
Chair, BE Graduate Committee



ARCHIVES

Development and analysis of an *in vitro* model of
inflammatory cytokine-mediated idiosyncratic drug hepatotoxicity

by

Maya Hasan

Submitted to the Department of Biological Engineering on August 10, 2007 in
Partial Fulfillment of the Requirements for the Degree of
Master of Engineering in Biomedical Engineering

Idiosyncratic drug reactions are a subset of adverse reactions frequently targeting the liver, which become obvious only in large sample populations. Drug-induced hepatotoxicity, occurring in a very small fraction of patients, poses a major challenge to pharmaceutical companies due to its unknown mechanism(s) of action and deficient models for study. *In vitro* model systems may have the potential to predict this liver injury by generating conditions possibly representing key processes involved, both directly and indirectly, in drug effects on cellular physiology. Our ultimate goal is to develop an *in vitro* model effectively mimicking certain relevant aspects of the *in vivo* response of the human liver. In our initial effort described herein, we have designed a novel cell-based system using alternatively in both a human hepatoma cell line and primary rat hepatocytes to study toxic effects in a background reflecting *in vivo* inflammatory conditions. This background incorporates bacterial lipopolysaccharide (LPS) administration along with inflammatory cytokines (tumor necrosis factor, interferon γ , interleukin- 1α , interleukin- 1β , and interleukin-6) previously shown to increase in LPS-administrated rats.

Our study began with an investigation of toxicities that are induced by combinations of five cytokines and LPS in HepG2 and C3A human hepatoma cell lines and in primary rat hepatocytes. Informed by the results of these experiments, we selected representative cytokine/LPS treatments and cell systems to examine drug-cytokine synergies *in vitro* and were able to identify multiple idiosyncratic hepatotoxins that induced synergistic toxicity in either the HepG2 cell line or primary rat hepatocytes. Finally, we measured the sensitization of these cell systems to a panel of these drugs, given an inflammatory background induced by an abbreviated set of cytokine treatments including four cytokines and LPS. Analysis of this multivariate drug-cytokine toxicity data set yielded a subset of representative cytokine treatments for future drug-cytokine synergy investigations. This subset will be used to characterize the differences between cell systems, including cultured human hepatocytes, and to hopefully develop a data-driven partial least squares regression model that predicts idiosyncratic liver injury. The implications are two-fold. First, this model could provide direction to pharmaceutical companies in focusing their drug discovery and development. Second, it could help physicians design better treatment plans for their patients.

Thesis Supervisor: Douglas A. Lauffenburger

Title: Whitaker Professor of Bioengineering, Chemical Engineering, and Biology; and
Director of the Biological Engineering Division

Acknowledgements

This thesis work would not have been possible without the guidance and support of my advisor, colleagues, friends, and family. Thanks to:

Douglas Lauffenburger for initially inviting me to join his lab, thereby providing me with a home and purpose in pursuing this research project. In my mind, he is the consummate advisor and a role model for both his students and other leaders in academia and industry.

Ben Cosgrove for teaching me how to do good, meticulous, and thorough science. His efforts are on every page of this thesis, and I can only hope that working with me has benefited him even a fraction of how much his mentorship has helped me.

Evi Farazi and Leonidas Alexopoulos for their collaborative efforts. Evi took me under her wing when I first joined the lab, and both have been excellent resources, critics, and sounding boards for discussion during the past year. The hepatocyte signaling network diagram on page 59 was also adapted from Leo's original.

Our collaborators at Pfizer, especially David de Graaf and Jim Xu, for their innumerable contributions to this project.

Bracken King for providing all the mutual information and joint entropy evaluations and figures presented in this work.

Members of the DAL lab, as well as my officemates in 56-353 and 56-379, for providing assistance or distraction, depending on what was necessary.

Those TAs, classmates, and partners, who made it possible for a biologist to enter the world of engineering.

My friends for reminding me that there is life beyond the big hood in TC Room B and the farthest bench, and that blisters from pipetting eventually go away.

My parents for supporting my decision to stay on at MIT and for encouraging me throughout this process.

Pfizer, Inc. and MIT's Cell Decision Process Center for funding this research.

Table of Contents

1	Introduction	Error! Bookmark not defined.
2	Materials and methods	11
2.1	Cell culture	11
2.1.1	Human hepatoma cell lines	11
2.1.2	Primary rat hepatocytes.....	12
2.1.3	Cytokines, LPS, and drugs.....	13
2.2	Assays	15
2.2.1	Rationale	15
2.2.2	LDH release assay.....	16
2.2.3	Effector caspase activity assay.....	17
2.2.4	Intracellular ATP assay.....	17
2.2.5	Calculating results.....	18
2.2.6	Multiplexing homogenous assays	18
2.3	Analytical techniques	19
2.3.1	Factorial analysis	19
2.3.2	Principal component analysis	22
2.3.3	Mutual information	23
2.3.4	Euclidean clustering.....	24
2.3.5	Drug-cytokine synergy calculations	24
3	6-cytokine/LPS multiplexing	26
3.1	Results from human hepatoma cell lines	26
3.2	Results from primary rat hepatocytes	28
3.3	Trends across the data set	30
3.4	Conclusions	33
4	Identifying drug-cytokine synergies	35
4.1	Rationale	35
4.2	Comparison of drug pairs across an inflammatory background	35
4.3	Drug-cytokine synergy calculations	43
5	5-cytokine/LPS multiplexing	46
5.1	Results from human hepatoma cell line	46
5.2	Results from primary rat hepatocytes	47
5.3	General trends across the data set	48
5.4	Further analysis	50
5.5	Conclusions	53
6	Discussion	55

7	Future Work	57
7.1	Primary human hepatocytes	57
7.2	Cellomics imaging	57
7.3	Intracellular signaling	57
8	References	60
9	Appendices	62
9.1	Appendix 1. Hepatocyte growth medium recipe.....	62
9.2	Appendix 2. Primary rat hepatocyte data from 6-cytokine/LPS multiplex ..	63
9.3	Appendix 3. HepG2 data from 5-cytokine/LPS multiplex	65
9.4	Appendix 4. Primary rat hepatocyte data from 5-cytokine/LPS multiplex ..	69

1 Introduction

Idiosyncratic drug reactions are a subset of adverse reactions that occur in a small fraction of patients; their development is hypothesized to be due to the genetic predisposition and environmental factors of an individual. Susceptibility to drug toxicity is difficult to predict in preclinical studies and clinical trials because of the limited sample sizes. Only when drugs hit the market do idiosyncratic reactions become obvious, frequently targeting the liver [Waring *et al.*, 2006]. Drug-induced liver disease is often serious, requiring liver transplantation, and is sometimes fatal; it accounts for about half of all cases of acute liver failure in the United States. In addition, hepatotoxicity (defined as cytotoxicity of the hepatocyte, the key functional cell of the liver) is both the leading cause of drug development failure during clinical trials and the leading cause of post-marketing warnings and withdrawals. It poses a major challenge because of its unknown mechanism and deficient models for study [Kaplowitz, 2005].

Preclinical animal toxicology studies usually fail to identify the risk of hepatotoxicity during clinical trials or post-marketing; a survey examining the ability of animal studies to predict human toxicities indicated that human hepatotoxicities had among the poorest correlations with regulatory animal toxicity tests [Xu *et al.*, 2004]. Cell-based assay systems during the discovery phase of preclinical drug development are now being used to probe the question of organ toxicity. According to Xu *et al.* [2004], *in vitro* systems should be used in parallel to explore the diverse mechanisms of liver injury. The predictive power of these systems should be greater for assays that assess early events in pathogenic sequences. Ideally, both the endpoints of such an assay and the drug

concentrations necessary to elicit those endpoints would mimic human clinical observations.

In culture, primary hepatocytes (either isolated from rodents or donated from human liver samples) have limited retention of many of the key differentiated functionalities necessary to properly study the metabolism and hepatotoxicity of a variety of drug compounds [Brandon *et al.*, 2003]. Moreover, human and rat hepatocytes express a different repertoire of cytochrome p450 and Phase II metabolic enzymes, making cross-species comparisons difficult. HepG2 cells and their subclone, C3A cells, are two commonly used human hepatoma cell lines¹. These human hepatoma cell lines and other human hepatocellular carcinoma cell lines, such as HepaRG and Huh-7, have even more significant loss of expression of the key hepatocyte-enriched metabolic enzymes and are thus often poor predictors of drug-related hepatotoxicity [Hewitt *et al.*, 2007]. However, even considering their deficiencies related to expression of hepatic enzymes and transporters, primary cell systems and human hepatoma cell lines still offer the key advantages of being scale-able to high-throughput approaches and tractable cell models of liver function for systems-level investigations.

Recent rodent models developed by Roth and colleagues suggest that one of the environmental factors that may determine an individual's susceptibility to idiosyncratic drug hepatotoxicity is underlying inflammation during drug administration. Such animal models employ administration of bacterial lipopolysaccharide (LPS) to mimic endotoxin exposure and induce inflammatory cytokine release both systemically and within the liver by resident liver macrophages (Kupffer cells). Roth and colleagues have shown that LPS-

¹ HepG2 and C3A cell lines are both of human hepatoma origin (although they are often incorrectly identified as of human hepatocellular carcinoma origin) and are curated by ATCC (www.atcc.org).

induced inflammation enhances liver sensitivity to classical (aflatoxin B1) and idiosyncratic (ranitidine, trovafloxacin) hepatotoxins at concentrations that alone have minimal effects, but does not sensitize the liver to non-idiosyncratic drug compounds of similar pharmacological functions [Barton *et al.*, 2000; Luyendyk *et al.*, 2006; Waring *et al.*, 2006]. What accuracy LPS-treated animal models will have in predicting human liver toxicity over a broad spectrum of compounds is uncertain, in part because animal models are inherently low-throughput and results from only a few sets of pharmacological compounds have been published to date. Additionally, the specific roles of the multiple molecular mediators of LPS-induced inflammation (extracellular cytokines and intracellular signaling molecules) in regulating the sensitizations to drug-induced liver toxicity have not been identified in these animal models, but have been preliminarily examined in Kupffer cell-hepatocyte coculture models [Tukov *et al.*, 2006].

Motivated by these efforts, we are working to develop an *in vitro* model to mimic the *in vivo* response of the liver to drugs upon LPS-related inflammation. In work described herein, we have designed a novel cell-based system utilizing both a human hepatoma cell line and primary rat hepatocytes to study the toxic effects of multiple idiosyncratic hepatotoxins in the presence of defined inflammatory cytokine environments. To mimic the *in vivo* inflammatory response to LPS administration, our cell systems were treated with multiple combinations of LPS and the inflammatory cytokines tumor necrosis factor (TNF), interferon- γ (IFN γ), interleukin-1 α (IL-1 α), interleukin-1 β (IL-1 β), and interleukin-6 (IL-6), which are shown to be upregulated within the liver in LPS-administered rats [Bergheim *et al.*, 2006]. Our *in vitro* model does not explicitly include the non-parenchymal cells, such as Kupffer cells, that mediate the liver's response to

LPS, but instead the role of these cells is reproduced through the addition of the previously mentioned inflammatory cytokines in cell culture experiments containing hepatocytes or hepatoma cells only.

Our study began with an investigation of cytotoxicities that are induced by combinations of these five cytokines and LPS² in two human hepatoma cell lines (HepG2 and C3A) and primary rat hepatocytes to select representative cytokine/LPS treatment conditions and cell systems for examination of drug-cytokine interactions *in vitro*. Informed by the results of these experiments, we set forth to identify whether synergies exist between the selected representative cytokine cocktail and multiple pharmacologic compounds classified as idiosyncratic hepatotoxins in inducing toxicity in either a human hepatoma cell line or primary rat hepatocytes. After identifying multiple idiosyncratic hepatotoxic drugs that exhibit synergy with a representative cytokine cocktail, we asked how this selected set of drugs sensitized both cell systems to a spectrum of cytokine treatment conditions (containing four cytokines and LPS). This multivariate drug-cytokine toxicity data set was then analyzed to identify a subset of cytokine combinations for future drug-cytokine synergy investigations in cultured human hepatocytes. It was also used to characterize the differences between cell systems that differ in species (primary rat versus primary human hepatocytes) and in transformation state (human hepatoma cells versus primary human hepatocytes) in this drug-cytokine co-treatment *in vitro* model. In future efforts, we hope to develop a data-driven partial least squares regression (PLSR) model, based on the canonical cue-signal-response methodology, to

² In this text, experiments with combinations of four cytokines and LPS will be referred to as “5-cytokine/LPS” experiments and those with combinations of five cytokines and LPS will be referred to as “6-cytokine/LPS” experiments.

predict idiosyncratic liver injury based on knowledge of how drug therapies affect hepatocyte signaling networks in the way of Miller-Jensen *et al.* [2007].

The implications of this work and future modeling efforts are twofold. First, this *in vitro* cellular model of inflammatory cytokine-mediated hepatotoxicity could identify potential hepatotoxins earlier in the drug development processes. Or, similarly, a predictive PLSR model could provide direction to pharmaceutical companies in focusing their drug discovery efforts away from compounds that would significantly affect cellular mediators of drug-cytokine toxicity synergies. Second, our work could help physicians design better treatment plans for their patients by stratifying patients into different drug treatment programs depending on their preexisting inflammatory conditions and based on knowledge of particular synergies that exist between candidate drugs and various inflammatory cytokine environments.

2 Materials and methods

2.1 Cell culture

2.1.1 Human hepatoma cell lines

On Day 1 of the 6-cytokine/LPS multiplex experiment, 100 μ L of HepG2 and C3A cells from human hepatoma cell lines were grown on 96-well, collagen I-coated, black plates with clear bottoms (BD) in lot-controlled USDA tested 10% fetal bovine serum (HyClone)-containing EMEM (ATCC) supplemented with 1% penicillin-streptomycin (Invitrogen) at 30,000 cells/well, such that they were confluent the next day. At this time the media was aspirated, and cells were treated with various cytokine/LPS combinations in the previously described media. LDH release and intracellular ATP were measured 24 and 48 hours following dosing.

The HepG2 plating protocol remained the same during subsequent experiments (Figure 1). However, on Day 2 the media used during seeding was aspirated, and 5 μ g/mL insulin (R&D Systems) was added to the cells in 100 μ L of serum-free media supplemented with antibiotics. On Day 3, cells were co-treated with various cytokine/LPS combinations and, in most cases, idiosyncratic and non-idiosyncratic drugs; these dosing solutions were administered in the same serum-free, insulin-containing media supplemented with antibiotics. Cells were dosed with cytokine/LPS combinations and drugs simultaneously so that drug exposure occurred at maximum cytokine/LPS stimulation. Hepatotoxicity was then assayed between 12 and 48 hours using *in vitro* toxicity assays.

Cells were regularly passaged on a biweekly basis. HepG2 and C3A cells between passages 45 and 60 were used in 6-cytokine/LPS multiplex experiments. HepG2 cells

from passage 12 were used in the experiment identifying drug-cytokine synergies, and cells from passage 14 were used in the 5-cytokine/LPS multiplex experiment.

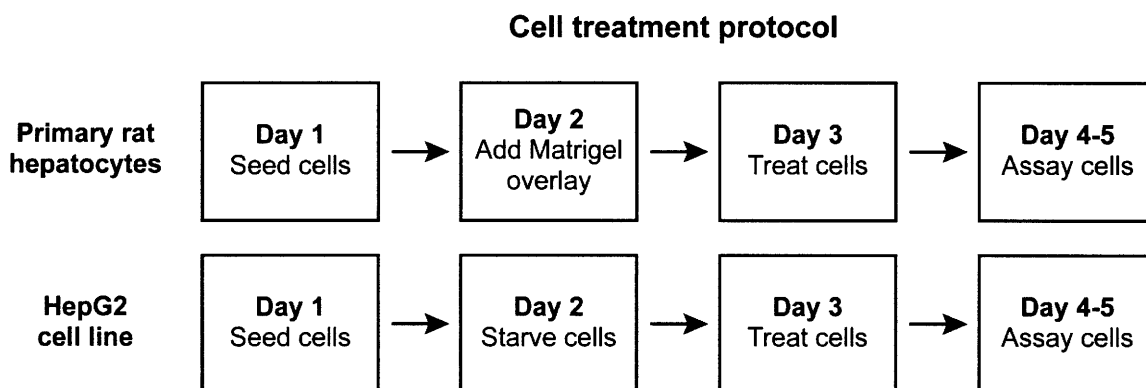


Figure 1. The timeline of experiments to identify drug-cytokine synergies and synergies across a 5-cytokine/LPS inflammatory landscape included growing primary rat hepatocytes in a collagen I-Matrigel sandwich configuration and serum-starving HepG2 cells.

2.1.2 Primary rat hepatocytes

Primary rat hepatocytes were isolated as described in Sivaraman *et al.* [2005].

Primary hepatocytes were isolated from male Fisher rats using a two-step collagenase procedure including multiple 50g centrifugations and a Percoll (Sigma) clarification centrifugation to increase hepatocyte purity and reduce contamination with non-parenchymal cells. Cell viability and yield were routinely greater than 90% and 300 million cells, respectively, as assessed by trypan blue exclusion staining using a Vi-CELL instrument (Beckman-Coulter). Purity of hepatocytes and non-parenchymal cells following Percoll isolation was assessed using a flow cytometry-based assay utilizing various liver cell type antigens as described in Cosgrove *et al.* [*in prep*]. Median cell type fraction values were as follows: 97% hepatocytes (cytokeratin-18⁺ cells), 0.4% Kupffer cells (ED2⁺ cells), 0.4% stellate cells (GFAP⁺ cells), and 0.2% sinusoidal endothelial cells (SE-1⁺ cells).

Primary rat hepatocytes were plated and cultured in hepatocyte growth medium (HGM) based on that described in Block *et al.* [1996]. HGM is a phenol red-free DMEM (Gibco)-based medium that contains necessary amino acids, sugars, trace metals, hormones, and 5 $\mu\text{g}/\text{mL}$ insulin (Sigma), but does not contain serum. In this work, the Block *et al.* HGM formulation was modified to contain 300 ng/mL trichostatin A (Sigma) and was made without EGF. See Appendix 1 for the full HGM formulation. Following Percoll isolation, primary rat hepatocytes were plated in 100 $\mu\text{L}/\text{well}$ HGM at 100,000 cells/cm^2 (32,000 cells/well) in 96-well, collagen I-coated plates (BD) (Figure 1). Four hours after plating, culture media was replaced with fresh HGM. On Day 2 of culture, an overlay of the reconstituted basement membrane solution Matrigel (BD) was added on top of the hepatocytes to mimic the complex extracellular environment and to maximize cellular differentiation. Ice-cold Matrigel (phenol red-free, growth factor-reduced) was added to ice-cold HGM to a final concentration of 0.25 mg/mL and was added at 100 $\mu\text{L}/\text{well}$ to freshly aspirated culture wells. Matrigel was allowed 24 hours to form a gel overlay before the media was aspirated on Day 3 and fresh HGM was added containing drugs and/or cytokines according to the treatment and assay protocols outlined for the HepG2 cells. For the preliminary 6-cytokine/LPS multiplex experiments, the Matrigel overlay step was omitted, and the hepatocytes were treated with cytokines in 100 $\mu\text{L}/\text{well}$ fresh HGM on Day 2 of culture.

2.1.3 Cytokines, LPS, and drugs

The 6-cytokine/LPS multiplex data set was collected using cytokines at the lowest concentrations listed in Table 1. In experiments in which cells were co-treated with both drugs and cytokines, dosing solutions were prepared to standardize administration using

cytokines at the highest concentrations listed in Table 1. Recombinant human and rat cytokines were obtained from R&D Biosystems and LPS serotype S1 from *E. coli* 0111:B4 was obtained from Sigma. Stock solutions of idiosyncratic and non-idiosyncratic drug pairs (Table 2) from the same pharmacologic class (Table 3) were prepared at 200× in 100% DMSO (Sigma) and diluted in insulin- and cytokine-containing HepG2 or primary rat hepatocyte media to 1× concentrations at 0.5% DMSO. As described in Section 4, a representative cytokine cocktail denoted “cytokine mix C” was used in a subset of the drug-cytokine co-treatment experiments; it contained 10 μg/mL LPS, 100 ng/mL TNF, 100 ng/mL IFN γ , and 20 ng/mL IL-1 α .

Table 1. Concentrations of cytokines and LPS used in this study.

Cytokine	Concentration (ng/mL)
LPS S1	10,000
TNF- α	100
IFN- γ	20-100
IL-1 α	10-20
IL-1 β	10-20
IL-6	2.5-20

Table 2. Drugs ordered from the following manufacturers or procured from collaborators at Pfizer.

Drug	Manufacturer
Aspirin	Sigma
Buspirone hydrochloride	Sigma
Cimetidine	Sigma
Clarithromycin	Sequoia Research
Entacapone	Sequoia Research
Famotidine	Sigma
Levofloxacin	Fluka BioChimika
Nefazodone hydrochloride	Sigma
Nimesulide	Sigma
Ranitidine hydrochloride	Sigma
Telithromycin	Sequoia Research
Tolcapone	Pfizer
Trovafloxacin	Pfizer

Table 3. Idiosyncratic and non-idiosyncratic drugs used in this study. The pharmacologic class of each is listed, along with its maximum concentration encountered by the liver. Those compounds in red have been identified as causing drug-induced liver injury (DILI) by our collaborators at Pfizer. Results from Roth and colleagues are summarized from Luyendyk *et al.* [2006] and Waring *et al.* [2006].

Compounds to investigate in drug-cytokine hepatotoxicity synergy model

Drug	100*C_{max} human plasma concentration (high end of “therapeutic window”)	Pharmacologic class	Synergy in LPS-administered animal model (Roth group)
Buspirone	0.5 μM	serotonin receptor inhibitor	<i>not reported</i>
Nefazodone	86 μM	serotonin receptor inhibitor	<i>not reported</i>
Clarithromycin	334 μM	antibiotic	<i>not reported</i>
Telithromycin	277 μM	antibiotic	<i>not reported</i>
Aspirin	552 μM	non-steroidal anti-inflammatory drug	<i>not reported</i>
Nimesulide	2108 μM	non-steroidal anti-inflammatory drug	<i>not reported</i>
Famotidine	30 μM	histamine H2-receptor antagonist	-
Ranitidine	142 μM	histamine H2-receptor antagonist	+
Cimetidine	1542 μM	histamine H2-receptor antagonist	<i>not reported</i>
Levofloxacin	1577 μM	antibiotic	-
Trovafloxacin	769 μM	antibiotic	+
Entacapone	393 μM	catechol-O-methyl transferase inhibitor	<i>not reported</i>
Tolcapone	2084 μM	catechol-O-methyl transferase inhibitor	<i>not reported</i>

Color key: *Compound not associated with liver injury*
Compound associated with idiosyncratic liver injury (DILI P2)

2.2 Assays

2.2.1 Rationale

We chose to multiplex several of Promega’s cell viability, cytotoxicity, and apoptosis assays to measure the endpoints during this screen of multiple drugs across inflammatory cytokine backgrounds. We could have instead used various imaging techniques or a variety of sub-lethal toxicity endpoint assays, but we found that the high-throughput nature of these lethal toxicity assays and their ease of use outweighed the benefits of the

former. These assays may be less informative than a flow cytometry-based apoptosis assay, for example, but they allowed us to collect a depth and breadth of data that would not have otherwise been possible and that discriminated between the many possible cytokine combinations.

2.2.2 LDH release assay

The CytoTox-ONE™ Homogenous Membrane Integrity Assay (Promega) was used to measure cytotoxicity by the release of lactate dehydrogenase (LDH), a stable cytosolic enzyme, into the surrounding medium upon cell lysis (Figure 2). It is a fluorometric method used to estimate apoptotic and necrotic cell death by loss of membrane integrity in a mixed population of viable and damaged cells. LDH released into culture supernatants is measured with a 10-minute coupled enzymatic assay driven by the presence of excess lactate and NAD^+ . LDH catalyzes the conversion of these substrates into pyruvate and NADH; the latter subsequently drives the diaphorase-catalyzed reduction of resazurin to produce fluorescent resofurin. Fluorescence is proportional to the number of lysed cells. In some cases, cell lysis reagent was added to positive control wells prior to the addition of CytoTox-ONE™ Reagent to generate a maximum LDH release control. Also, stop solution was not added.

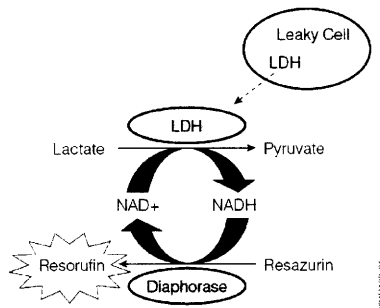


Figure 2. LDH substrate of coupled reduction-oxidation reactions resulting in the production of fluorescent resorufin. LDH is released by cells suffering a loss of membrane integrity. Supplying the excess substrates lactate, NAD^+ , and resazurin, ensures fluorescence is proportional to the number of necrotic cells [Promega].

2.2.3 Effector caspase activity assay

The Caspase-Glo[®] 3/7 Assay (Promega) is a luminescent method used to measure apoptosis in adherent cells. After causing cell lysis, it provides the luminogenic substrate DEVD-aminoluciferin for caspase-3/7 cleavage and luciferase to generate a luminescent signal by consuming the liberated free aminoluciferin (Figure 3). The resulting luminescence is proportional to caspase-3/7 activity. Samples were incubated for one hour.

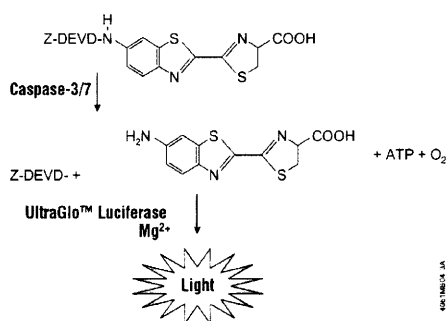


Figure 3. Luminescent signal generated following caspase-3/7 cleavage of DEVD-aminoluciferin. Cleavage of the luminogenic caspase-3/7 substrate releases free aminoluciferin into the surrounding medium for luciferase action [Promega].

2.2.4 Intracellular ATP assay

The CellTiter-Glo[®] Luminescent Cell Viability Assay (Promega) is a method of measuring cell viability via its correlation with intracellular ATP. The Cell-Titer-Glo[®] Reagent causes cell lysis and the release of ATP into the surrounding culture medium;

upon loss of membrane integrity, the cell loses its ability to synthesize additional ATP. The reagent simultaneously inhibits endogenous ATPases and provides the reactants for a luminescent reaction to measure ATP.

2.2.5 Calculating results

The average value of culture medium background fluorescence or luminescence was subtracted from all experimental wells. Experimental values were then normalized to the average signal from untreated control wells (containing no cytokines and 0.5% DMSO when appropriate). Assay data is therefore presented in Relative Fluorescence (RFU) or Luminescence Units (RLU).

2.2.6 Multiplexing homogenous assays

These assays were used in parallel such that more than one data set was collected from the same sample. In cases in which the intracellular ATP assay was multiplexed with the LDH release assay, all media was transferred to a separate assay plate for the LDH release assay and 100 μ L of fresh media was added to each well on the original assay plate. The ATP release assay protocol was then followed as recommended by the manufacturer. Alternatively, 50 μ L of culture supernatant was removed to a separate white assay plate (Nunc) to gather cytotoxicity data using the LDH release assay, leaving the original assay plate available for caspase activity measurements of apoptosis.

When multiplexing assays it is especially important to understand what a given assay is measuring and how it is correlated with cell viability, cytotoxicity, or apoptosis. It is also important to understand the kinetics of the cell death process to inform decisions like the choice of assay endpoint. For example, cells undergoing rapid necrosis, characterized by loss of membrane integrity and metabolic shutdown, do not express apoptotic markers.

On the other hand, apoptotic cells transiently express those markers before undergoing secondary necrosis *in vitro*.

2.3 Analytical techniques

2.3.1 Factorial analysis

In this study we first performed a battery of experiments to measure the effects of, and identify the synergies between, five cytokines and LPS on hepatocellular viability, cytotoxicity, and apoptosis. Later, we set forth to detect synergies between five inflammatory agents and a variety of idiosyncratic and non-idiosyncratic drug compounds. In both cases, we used a full p^q factorial design, where q is the number of variables (factors) and p is the number of levels at which the variable is tested; there were $2^6 = 64$ combinations in the first case and $2^5 = 32$ in the second. The concentrations at which these cytokines were tested are explained in Section 2.1.3. This analytical technique identifies main effects and interactions and informs further experimentation. In this case, it measured the additive or subtractive effect of any single or group of conditions on toxicity. The following explanation was adapted from Box *et al.* [1978].

The main effect of a variable is its average effect on the response, regardless of the levels of the other variables. In our two-level factorial design for six inflammatory agents, the main effect of variable i is given by

$$\text{main effect} = \bar{y}_{i, \dots} - \bar{y}_{\dots}$$

where $\bar{y}_{i, \dots}$ is the average measured outcome in the presence of a given cytokine and \bar{y}_{\dots} is the average value in its absence. Each of the calculated main effects is therefore dependent on all 64 of the responses. Also, each is determined with the precision of 32 replicated experiments.

In addition to more precisely measuring the additive effects of variables on outcomes compared to an experimental method in which one variable is varied at a time, this analytical technique has the added benefit of calculating potentially synergistic interactions that may result from the presence of multiple variables in a system using fewer observations than the one-factor-at-a-time method. For variables i and j in our 2^6 factorial design, the $i \times j$ interaction is

$$i \times j \text{ interaction} = \frac{\bar{y}_{ij\dots} - \bar{y}_{i\dots} - \bar{y}_{\dots j} + \bar{y}_{\dots\dots}}{2}$$

or half the difference between the average effect of variable i in the presence and absence of j . By extension, for variables i through m , the six-factor interaction is

$$i \times j \times k \times l \times m \times n = \frac{y_{6/6} - y_{5/6} + y_{4/6} - y_{3/6} + y_{2/6} - y_{1/6} + y_{0/6}}{32}$$

where, for example, $y_{3/6}$ represents all the outcomes in the presence of only three of the six inflammatory agents. It is important to remember that each interaction can be defined as half the difference between two averages, and that the outcome in the presence of all variables, y_{ijklmn} , has a positive effect on any main effect or interaction.

Before the main effects and interactions can be interpreted, the associated standard errors must be calculated. With replicated observations, the pooled estimate of run variance is

$$s^2 = \frac{\sum_{i=1}^g (n_i - 1) s_i^2}{\sum_{i=1}^g (n_i - 1)}$$

where g is the number of conditions; and n_i is the number of replicates, $n_i - 1$ is the degrees of freedom, and s_i^2 is an estimate of the variance σ^2 , for the i th condition. Each effect or interaction is the difference between two averages, $\bar{y}_+ - \bar{y}_-$, so the variance v of each effect or interaction is

$$v = \left(\frac{1}{n_+} + \frac{1}{n_-} \right) \sigma^2$$

where n_+ is the total number of replicates used to calculate \bar{y}_+ and n_- is the total number of replicates used to calculate \bar{y}_- . The estimated standard error of each main effect or interaction is calculated by

$$\text{standard error} = \pm \sqrt{v}$$

Factorial analysis calculations were performed on fold change versus no cytokine control data in all cases. The guidelines governing the interpretation of factorial effects tell us that main effects cannot be interpreted individually if either plays a role in significant higher-order interactions.

Statistical significance of each factorial effect or interaction \bar{y}_{ij} was evaluated using a one-sample, two-tailed t -test. A 95% confidence interval for each effect or interaction was calculated using its standard error v and an appropriate critical t -value t^* , which was calculated as a function of the number of biological replicates n and the desired statistical confidence level α .

$$CI_{95\%} = \bar{y}_{ij} \pm t_{n-1, \alpha}^* \cdot v$$

A Bonferroni correction to the statistical confidence level was used to account for multiple comparisons because the significance of multiple effects and interactions were

evaluated simultaneously. For example, in the evaluation of the 5-cytokine/LPS/drug co-treatment experiments, five biological replicates were used and 31 different effects or interactions were evaluated. Thus, a statistical confidence level of $\alpha = 0.05/31 = 0.0016$ was used, yielding a critical t -value of $t_{4,0.0016}^* = 7.56$. If the 95% confidence interval of a given effect or interaction did not contain zero (the null hypothesis of no effect), then the effect or interaction was deemed statistically significant.

2.3.2 Principal component analysis

A principal component analysis (PCA)-based data mapping approach was used to examine co-variations in the 6-cytokine/LPS combinatorial toxicity data set collected in the three hepatocyte cell systems. A data matrix was constructed containing rows representing the 64 unique cytokine treatment combinations and 12 columns representing both discretized classifications of the six cytokine treatment variables and the measured LDH release values for HepG2 cells, C3A cells, and primary rat hepatocytes at 24 and 48 hours post-treatment. The cytokine treatment columns were formulated as discretized treatment concentrations with '0' representing no cytokine and '1' representing a cytokine that was included in a given treatment. The LDH release data columns were formulated as fold change values separately normalized for each cell type and time point (as plotted in Figures 4 and 6). Thus, the values in each row of the data matrix could project as a series of coordinates in a multi-dimensional cytokine treatment classification- and toxicity data-space [Janes *et al.*, 2006]. A PCA algorithm was implemented (SIMCA-P, U-Metrics) to map the multi-dimensional cytokine treatment-/toxicity outcome-space onto a set of principal component axes to capture a significant amount of the co-variation in the data matrix. Preceding PCA mapping, each column of the data matrix was

separately mean-centered and variance-scaled following accepted data pre-processing methods for disparate data types [Geladi *et al.*, 1986]. A two-component PCA map was obtained that captured 43% of the entire variation in the data set (as measured by cumulative R^2) with the first and second principal component containing 30% and 13% of the variation, respectively. Additional principal components provided non-significant additions in capturing variation in the data matrix (R^2) and/or cross-validated predictions based on the principal component mapping (Q^2) (data not shown). PCA loadings for each column of the data matrix are plotted in Figure 7 and represent how data from each cytokine treatment classifier or LDH outcome measurement map onto the two principal component axes. Similar patterns of loadings onto these two principal component axes for sets of treatment classifiers or cell systems indicate related co-variation across the entire set of 64 unique cytokine treatments.

2.3.3 Mutual information

In the 6-cytokine/LPS experiments, cytokine treatment variables whose presence or absence were most informative of the six measured LDH release outcomes (HepG2, C3A or primary rat hepatocyte cells at 24 or 48 hours) were computed [King and Tidor, *in prep*]. Cytokine treatment variables were scored for information content by estimating the mutual information between the cytokine variable and the set of outputs, using a second order joint entropy approximation.

To identify characteristic subsets of the 32 cytokine conditions in the 5-cytokine/LPS/drug experiments, 1000 subsets ranging in number of included unique cytokine treatments from 4 to 32 were chosen at random for all possible permutations. These subsets were scored by estimating the joint entropy of all drug and DMSO control

treatment responses. Caspase 3/7 activity data in the HepG2 cells at 24 hours post-treatment was used as a test data set for this approach. The subset of each size with the highest computed joint entropy was chosen as the most representative.

2.3.4 Euclidean clustering

Hierarchical clustering was conducted to identify and distinguish clusters of toxicity outcomes based on cytokine treatment conditions, cell system, and/or drug co-treatments. For the 6-cytokine/LPS combinatorial experiments, LDH release data from HepG2 cells, C3A cells, and primary rat hepatocytes at 24 and 48 hours post-treatment was normalized to fold change (separately for each cell system and time point) and subjected to hierarchical clustering. Hierarchical clustering was performed in Matlab (Mathworks) using a Euclidean distance metric with linkages evaluated by the unweighted pair-group method with arithmetic averages [D'haeseleer, 2005]. Clustering was separately conducted on the 64 unique cytokine treatments and the six cell systems/time points. For the 5-cytokine/LPS combinatorial experiments in the presence of drug co-treatments, clustering was performed as described above for a representative data set (caspase 3/7 activity at 24 hours post-treatment in HepG2 cells) and was used to distinguish clusters of both cytokine treatment conditions and drug co-treatments.

2.3.5 Drug-cytokine synergy calculations

Synergistic interactions between drugs and inflammatory agents are those effects that are greater than the sum of their individual effects. Therefore the cytotoxic effect of cytokine mix C alone as measured by LDH release was added to each toxicity value of drug alone across the range of tested concentrations at three time points in both HepG2s and primary rat hepatocytes. These projected dose-response curves describe the toxicity

that would be predicted for each drug if there was a purely additive cytotoxic effect between the compound and cytokine mix C. Drugs that synergized with the inflammatory cytokine background were easily identifiable using this intuitive technique since their measured toxicity values exceeded those predicted by simple addition. For all combinations of drug, cell systems, and time points, the drug concentration that exhibited the greatest synergistic toxicity above the predictive additive toxicity was identified and reported in Table 4.

3 6-cytokine/LPS multiplexing

3.1 Results from human hepatoma cell lines

A number of general trends become obvious upon inspecting the data set collected from the human hepatoma cell lines (Figures 4, 5). Unfortunately, however, the limited number of replicates in this cell line experiment makes the statistical significance of the data subject to skepticism.

Very little cytotoxicity was measured by the LDH release assay across the spectrum of cytokine backgrounds in HepG2s at 24 hours, an observation reiterated by the negligible factorial effects calculated for the time point (Figure 4). In the presence of a single cytokine, only minimal cell death was seen in either cell line at both time points; in contrast, the most LDH release was measured in the presence of some of the highest-order cytokine combinations. The C3A cell line exhibited a similarly modest level of cell death as measured by the LDH release assay at 24 hours, with a few notable exceptions in the presence of three- or higher-order cytokine combinations. The common inclusion of LPS in these apparently cytotoxic cytokine combinations explains the strong positive factorial effect of the bacterial endotoxin. LPS treatment co-varied with the LDH release data from the C3A cells at 24 hours in the PCA map (Figure 7). More cytotoxicity was evident at 48 hours in both cell lines; by inspection it seems that IL-1 α was a common denominator among the most cytotoxic cytokine combinations in HepG2s, just as the presence of TNF and IFN γ seem to affect cell death in C3As (Figure 4).

Cell viability data from the intracellular ATP assay was very noisy and did not correlate with increased LDH release (Figure 5). No clear trends were evident and the fold change assay values only varied across a twofold range; this variability was

propagated into the factorial analysis. The unreliable data may result from the effects of metabolic variation induced by cytokine treatment.

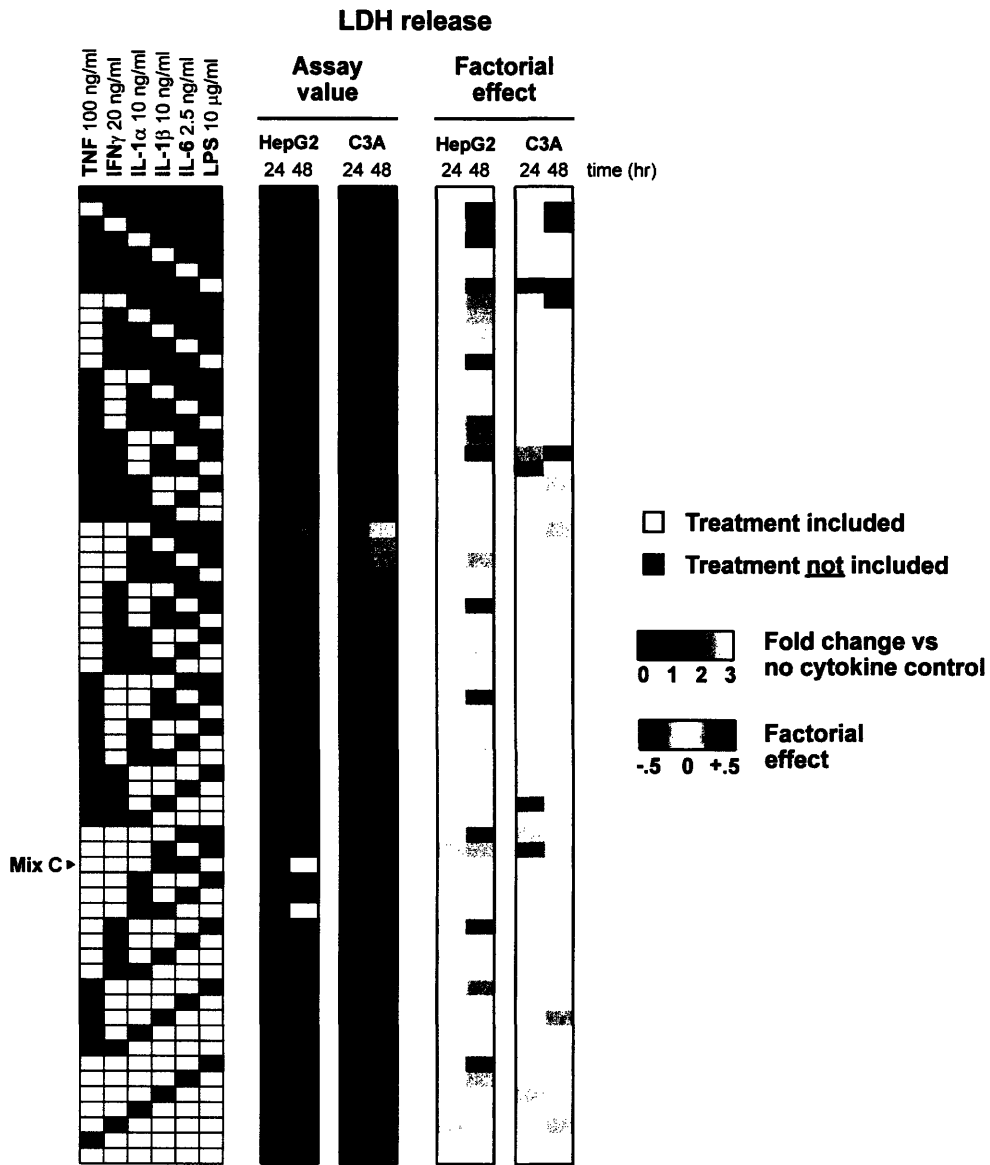


Figure 4. LDH release data set from the 6-cytokine/LPS multiplex experiment in both human hepatoma cell lines at two time points. Cytokine mix C is identified in the treatment matrix, and mean assay values are presented as fold change versus the no cytokine control.

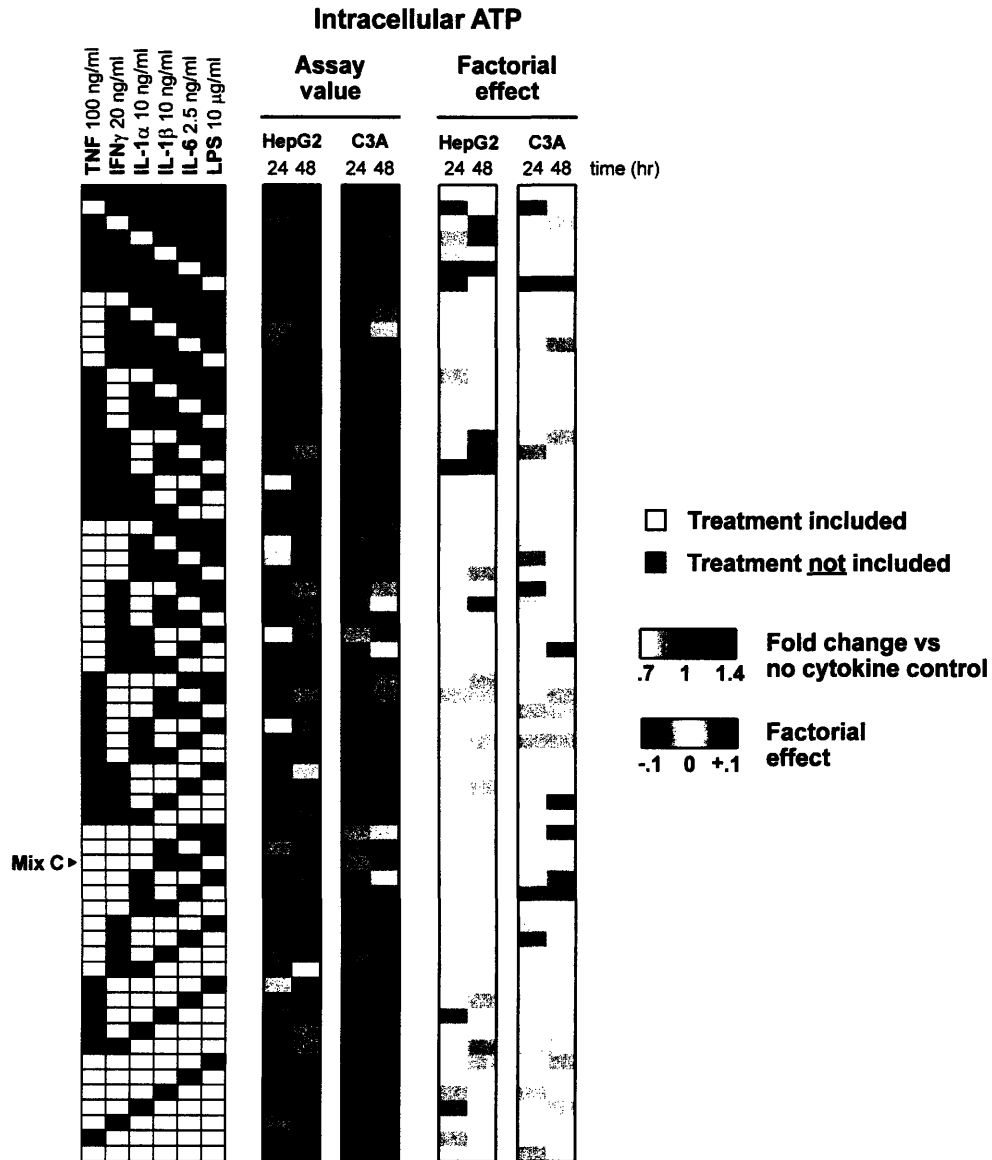


Figure 5. Intracellular ATP data set from the 6-cytokine/LPS multiplex experiment in both human hepatoma cell lines at two time points. Cytokine mix C is identified in the treatment matrix, and mean assay values are presented as fold change above the no cytokine control.

3.2 Results from primary rat hepatocytes

Primary rat hepatocytes underwent only background levels of apoptosis at 24 hours according to the caspase activity assay, and the LDH release assay revealed moderate cytotoxicity with higher-order cytokine combinations, a trend heightened at 48 hours (Figure 6). At 24 hours, the factorial effects as determined by both caspase 3/7 activity and LDH release assays revealed minimal meaningful main effects or multi-factor

interactions. In fact, none of the factorial effects calculated from this primary rat hepatocyte data set are statistically significant (Figures A1, A2). Qualitatively, however, it would seem that hepatocyte apoptosis was highly correlated with the presence of either TNF or IL-1 α at 48 hours, an observation supported by the strong positive factorial effects of these two cytokines (Figure 6). It is interesting that the main effect of IFN γ at 24 hours was amplified at 48 hours and that this cytokine also appeared in the notable two-factor interaction with LPS at this later time point. Importantly, only the IFN γ \times LPS interaction could be subject to interpretation (Section 2.3.1) if the results of this factorial analysis were, in fact, statistically significant.

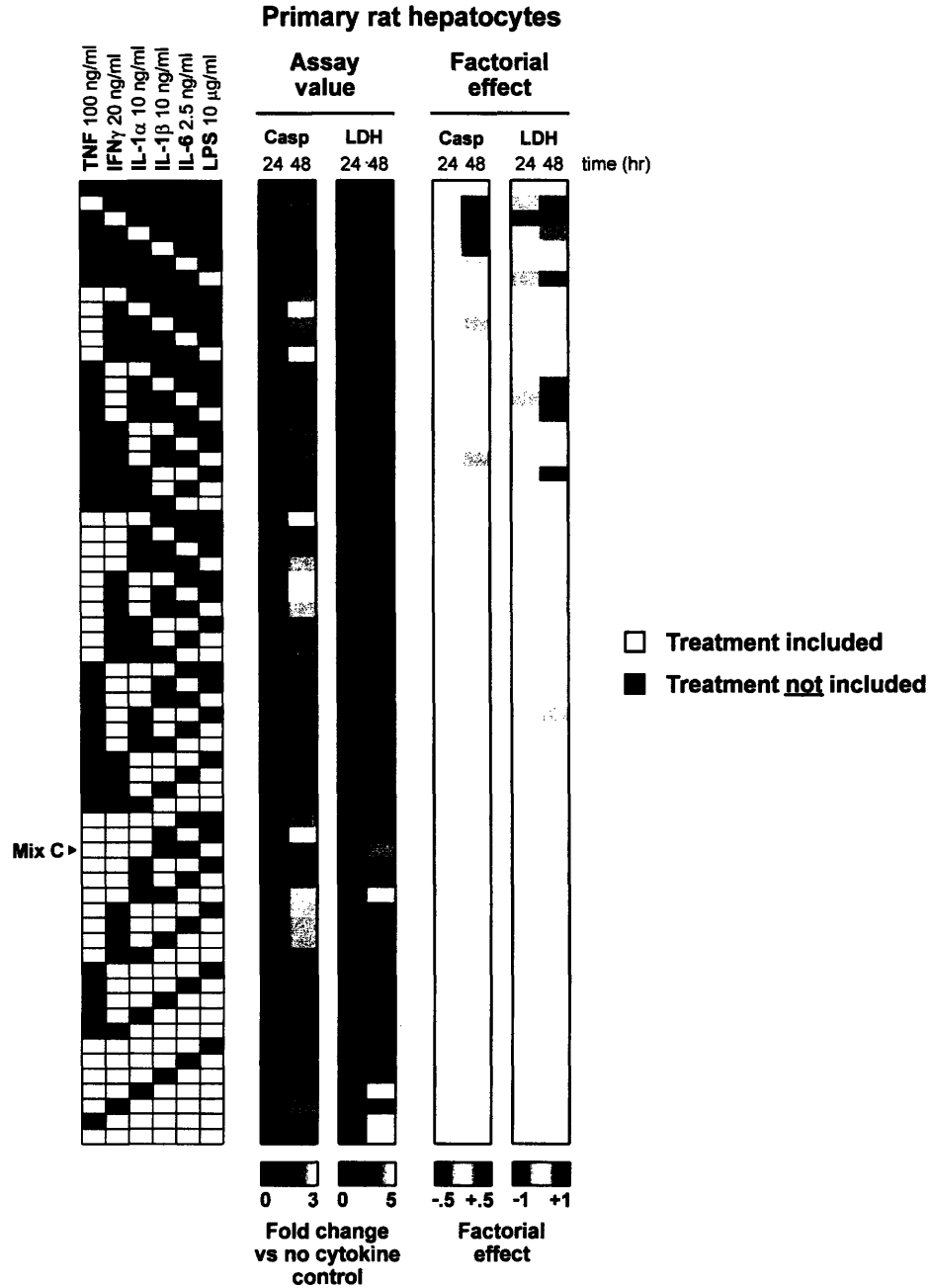


Figure 6. Caspase 3/7 activity and LDH release data sets from the 6-cytokine/LPS multiplex experiment in primary rat hepatocytes at two time points. Cytokine mix C is identified in the treatment matrix, and mean assay values and factorial effects are presented.

3.3 Trends across the data set

According to the PCA plot of the first two principal components, the LDH outcomes strongly impact the model, as evidenced by their distance from the origin, while the cytokines, especially IL-6 and IL-1 β , seem to have little effect on cytotoxicity (Figure 7).

The 48 hour data from all three hepatocyte cell systems group together in the PCA plot as outcomes with similar co-variations in LDH release. The five cytokines also appear to co-vary more closely with each other than with LPS.

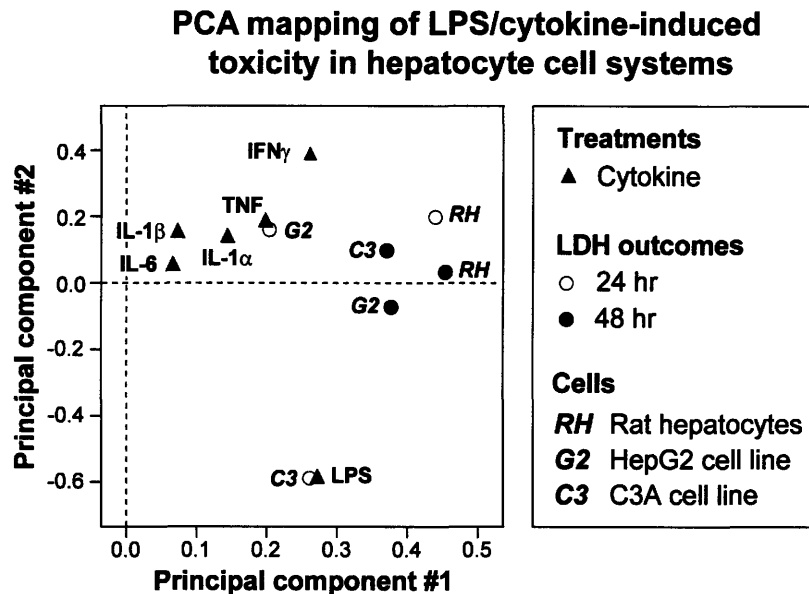


Figure 7. PCA plot of LDH release data sets from both the human hepatoma cell lines and primary rat hepatocytes. The first component explains 30% of the variation and the second component 13%. The C3A data at 24 hours is strongly co-varied with the LPS treatment in both principal components.

In addition, a Euclidean clustering of the same LDH release data set greatly distinguished the cytokine-induced cytotoxicity in primary rat hepatocytes at 48 hours from the other combinations of cell system and time point, as the primary rat hepatocytes demonstrated a far greater cytotoxic response than the other cell systems at either time point (Figure 8). Clustering also illustrated the similarity between LDH release outcomes of HepG2s and C3As. LDH release generally increased in the presence of higher-order cytokine combinations, as discussed earlier. In particular, we identified cytokine mix C (TNF, IFN γ , IL-1 α , and LPS) as the least cytotoxic cytokine combination among the most cytotoxic combinations grouped together at the highest level of clustering. A mutual information analysis of the same LDH release cytotoxicity data set revealed that LPS

treatment was the most informative of the entire data set, followed by IFN γ , IL-1 α , TNF, IL-6, and IL-1 β (Figure 9).

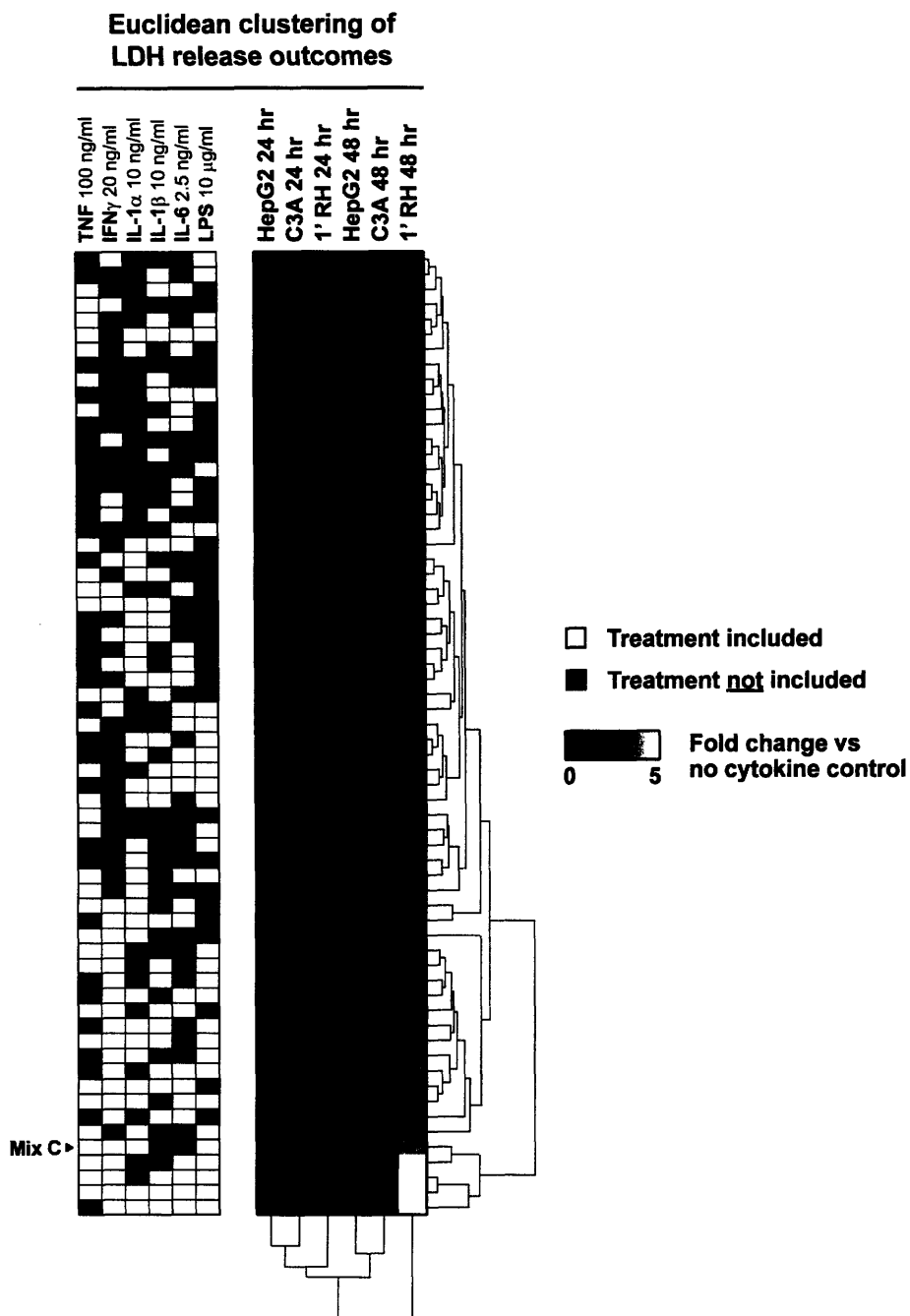


Figure 8. Euclidean clustering of LDH release data sets from both the human hepatoma cell lines and primary rat hepatocytes. Cell systems clustered by time point, with the HepG2 cell line and its subclone clustering closely at both 24 and 48 hours. The primary rat hepatocyte data set from 48 hours was by far the most cytotoxic. Cytokine mix C is identified as the least cytotoxic cytokine combination among the combinations that exhibited the most cytotoxicity and clustered together at the highest level.

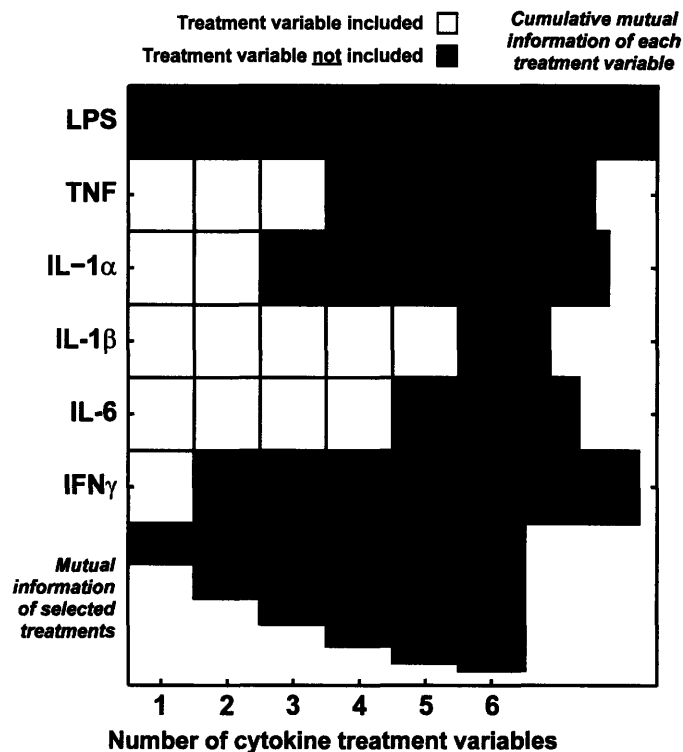


Figure 9. Mutual information evaluation to choose the most informative cytokines. A second-order joint entropy approximation was used [Bracken King].

3.4 Conclusions

To maximize our efficiency in subsequent experiments, we chose to only continue testing the hepatotoxic responses of HepG2s and primary rat hepatocytes. Keeping in mind that our ultimate goal was to identify a cell system that closely mimics an *in vivo* human liver, it seemed prudent to maintain the use of at least one of the human hepatoma cell lines. Clustering illustrated the similarity between LDH release outcomes of HepG2s and C3As, which would be expected since C3As are a HepG2 subclone (Figure 8). To capture the greatest variability across the cell systems, we decided to keep using the HepG2 cell line, which clustered farthest from the primary rat hepatocytes at each time point.

Clustering of the 64 cytokine treatment combinations in order of increasing toxicity across the outcomes was also informative (Figure 8). Cytokine mix C was chosen for use

in subsequent experiments due to its sub-maximal hepatotoxic effects; our aim was to observe drug-cytokine synergies across a range of drug concentrations. The absence of IL-6 and IL-1 β from this combination is reminiscent of their minimal effect on cytotoxicity as highlighted in the PCA and mutual information results (Figures 8, 9). In fact, mutual information quantitatively substantiated our decision to eliminate IL-1 β from future experiments (Figure 9). Our decision was further supported by the biology; both IL-1 α and IL-1 β bind to the same receptor (IL-1R), eliciting similar cell signaling responses in hepatocytes, though often with differing potency depending on other co-stimulations [Luedde *et al.*, 2006].

4 Identifying drug-cytokine synergies

4.1 Rationale

It was important to identify the concentration of each drug which best synergized with a representative inflammatory cytokine background (cytokine mix C) to cause cytotoxicity in both HepG2s and primary rat hepatocytes for use in the 5-cytokine/LPS multiplex experiment. To achieve this goal, we compared the dose-response curves of drug pairs at the same molar concentration, as opposed to at equivalent multiples of their C_{max} values (maximum plasma drug concentrations in human administration). Scaling relative to the C_{max} values was avoided because these could differ drastically for any given pair of drugs, due to differences in compound efficacy and pharmacodistribution (Table 3). Also, testing each drug pair at the same molar concentration provides more comparable data in an *in vitro* system and is more applicable in a model trained to identify idiosyncratic hepatotoxicity during laboratory development, prior to clinical testing. As reported in Table 3, $100 \cdot C_{max}$ values provide an estimate of the worst-case liver exposure and exist at the high end of the “therapeutic window,” or the dose range that elicits therapeutic effects without causing toxicity alone. Preliminary experiments were used to inform the concentration range that was tested in both cell systems using LDH release and caspase activity assays at three time points.

4.2 Comparison of drug pairs across an inflammatory background

Cytotoxicity and apoptosis were measured spanning a range of drug concentrations at three time points in both cell systems. Only LDH release measurements were considered in identifying the optimal drug concentration for each analogous pair since the LDH release assay captures both apoptotic and non-apoptotic cell death.

Nefazodone, the idiosyncratic drug of the serotonin receptor inhibitor drug pair, showed clear drug-cytokine synergy at about 75 μM in both cell systems at 24 hours (Figure 10). This synergy was also evident at 48 hours in the primary rat hepatocytes. In HepG2s, the earlier onset of synergistic cytotoxicity may explain the decrease in measured LDH release at 48 hours; released LDH has a half-life of approximately 9 hours in the surrounding medium. The non-idiosyncratic analog buspirone exhibited minimal toxicity, regardless of an inflammatory cytokine background (Figure 10).

In the clarithromycin-telithromycin drug pair, it was interesting that clarithromycin displayed cytokine synergies at about 175 μM (Figure 11). Although clarithromycin was included in this study as telithromycin's non-idiosyncratic analog, it is also associated with idiosyncratic liver injury, although to a lesser extent. It caused synergistic hepatotoxicity at 24 and 48 hours in both cells systems. On the other hand, telithromycin did not appear to cause this same toxicity, and instead somewhat irregular dose-response curves were measured at both later time points (Figure 11). A hypothesis for this potentially unreliable data is discussed in Section 6.

Although both aspirin and nimesulide never demonstrated clear drug-cytokine synergy in the primary rat hepatocytes (nimesulide-mediated effects seem to dominate), nimesulide did induce synergistic toxicity at about 450 μM in the human hepatoma cell line at 24 hours (and to a lesser extent at 12 hours as well) (Figure 12). These effects had faded by 48 hours, similar to nefazodone. No aspirin-cytokine synergy was observed in HepG2 cells.

In contrast, ranitidine-cytokine synergy was measured by LDH release at 48 hours in primary rat hepatocytes (and to a lesser extent at 24 hours), but not in the cell line (Figure

13). This comes with the caveat that this synergy was observed at about 450 μM ($317 \cdot C_{\text{max}}$), a far higher concentration than is probably physiologically relevant. Also, similar to the clarithromycin-telithromycin drug pair, it was the non-idiosyncratic analog that displayed drug-cytokine synergy. However, ranitidine is also associated with liver injury, although to a lesser extent than cimetidine, and tested positive for hepatotoxicity in Roth's rat model (Table 3). Famotidine, the histamine H₂-receptor antagonist analog used by Roth, will probably be used as the non-idiosyncratic analog to ranitidine in future experiments with this class of compounds.

Trovafloxacin is another compound considered to be an idiosyncratic hepatotoxin according to the Roth model. It too showed clear drug-cytokine synergy at about 450 μM in both cell systems at all time points, most notably at 24 hours (Figure 14). In addition, it caused a much higher level of measured cytotoxicity in the HepG2 cell line compared to primary rat hepatocytes than was seen for any of the other drugs. To compare, its non-idiosyncratic analog levofloxacin exhibited negligible synergy across the board, as measured by LDH release (Figure 14).

The pair of catechol-O-methyl transferase inhibitors, entacapone and tolcapone, which proved fickle during preliminary experiments, once again did not show clear drug-cytokine synergy (Figure 15). These drugs were tested at high molar concentrations due to their relatively high $100 \cdot C_{\text{max}}$ values, possibly explaining their poor solubility. Also, like telithromycin, these drugs produced potentially-unreliable dose-response curves that may have been caused by unknown off-target effects.

Buspirone - Nefazodone

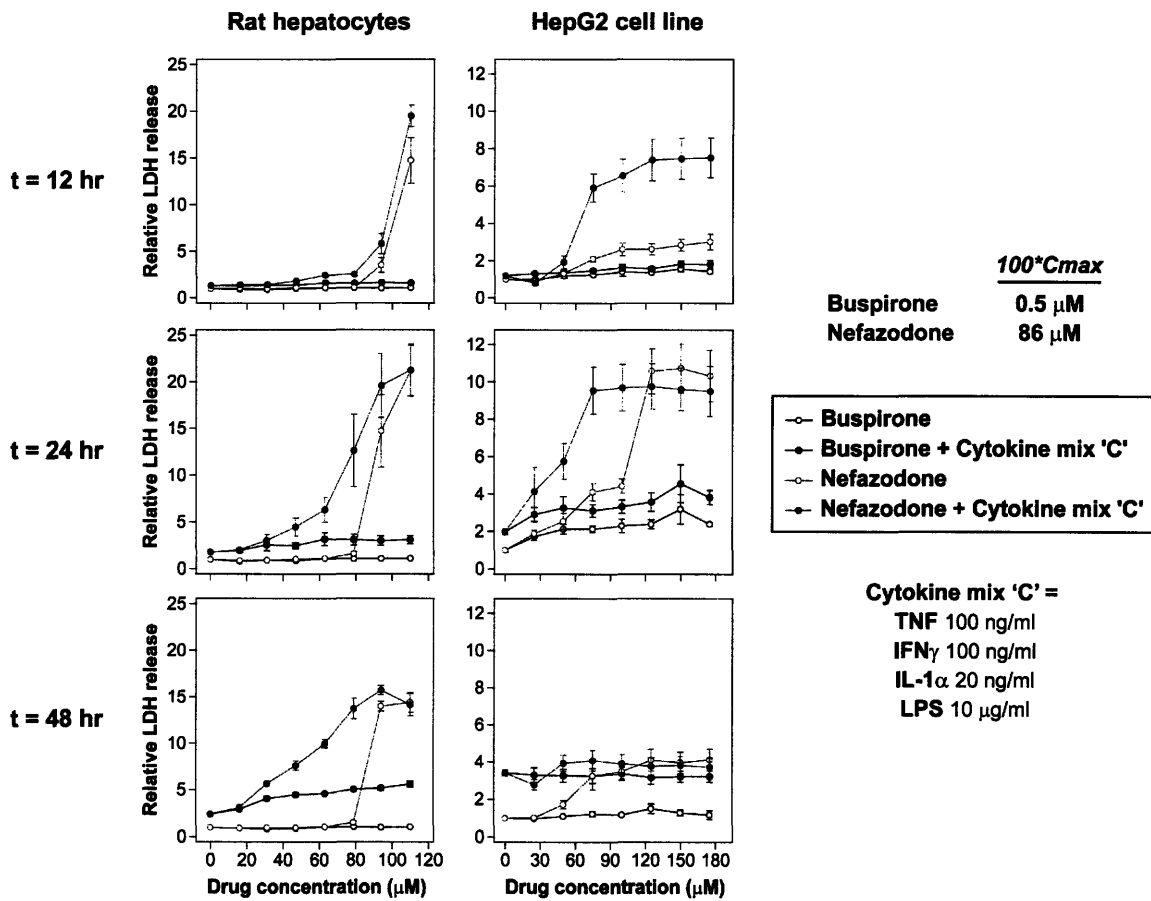


Figure 10. Dose-response curves of the buspirone-nefazodone drug pair from the mean LDH release data in both cell systems at three time points. Nefazodone showed clear drug-cytokine synergy around 75 μ M at 24 hours in HepG2s and primary rat hepatocytes. Error bars represent the standard error across four or more biological replicates.

Clarithromycin - Telithromycin

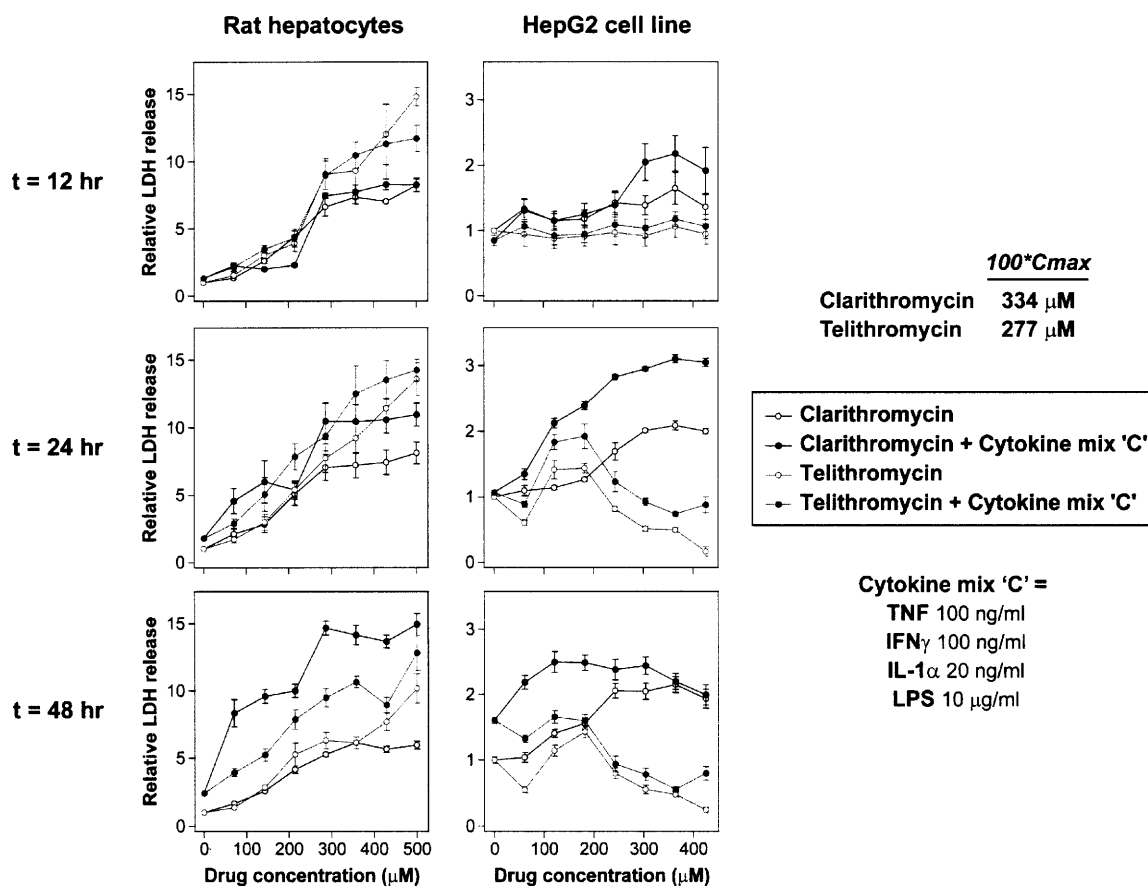


Figure 11. Dose-response curves of the clarithromycin-telithromycin drug pair from the mean LDH release data in both cell systems at three time points. Clarithromycin showed clear drug-cytokine synergy around 175 μM at 24 and 48 hours in HepG2s and primary rat hepatocytes. Error bars represent the standard error across four or more biological replicates.

Aspirin - Nimesulide

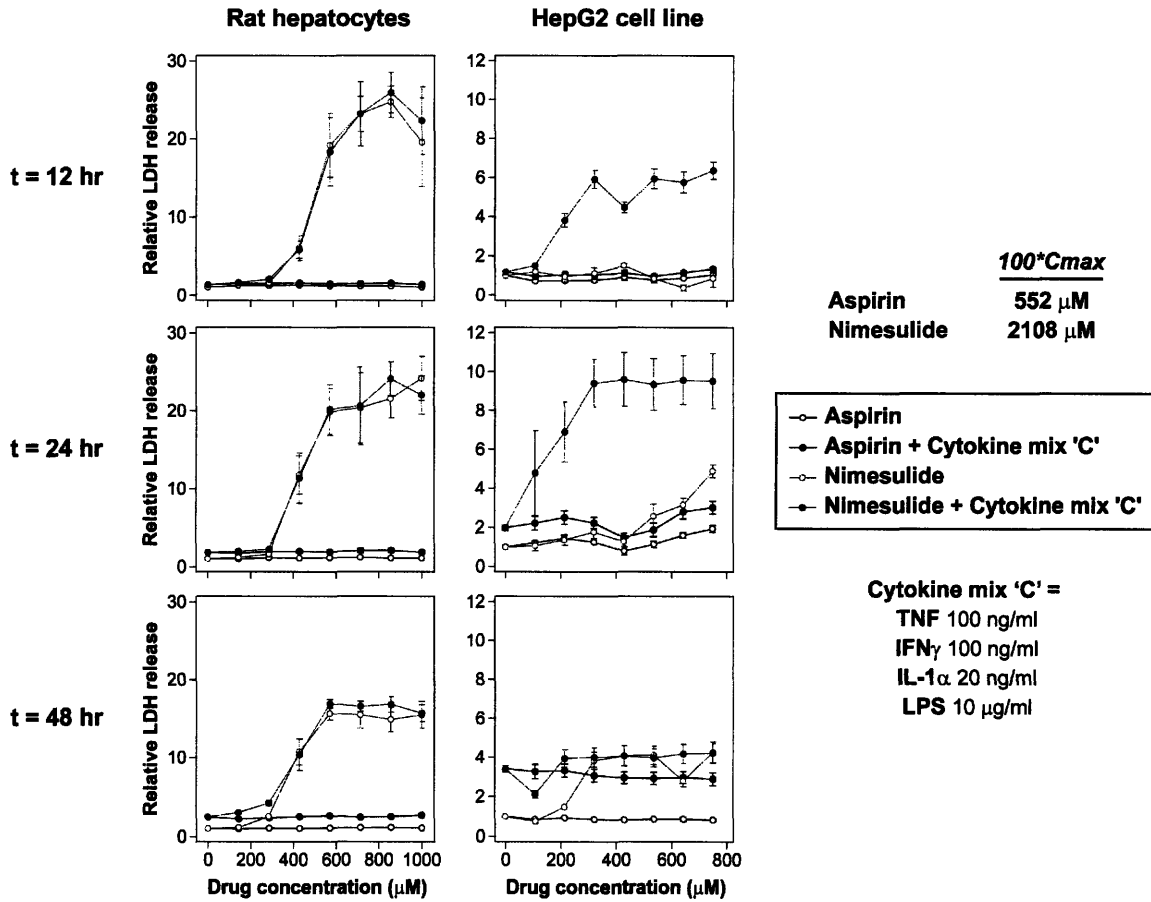


Figure 12. Dose-response curves of the aspirin-nimesulide drug pair from the mean LDH release data in both cell systems at three time points. Nimesulide showed clear drug-cytokine synergy around 450 µM at 24 hours in HepG2s. Error bars represent the standard error across four or more biological replicates.

Ranitidine - Cimetidine

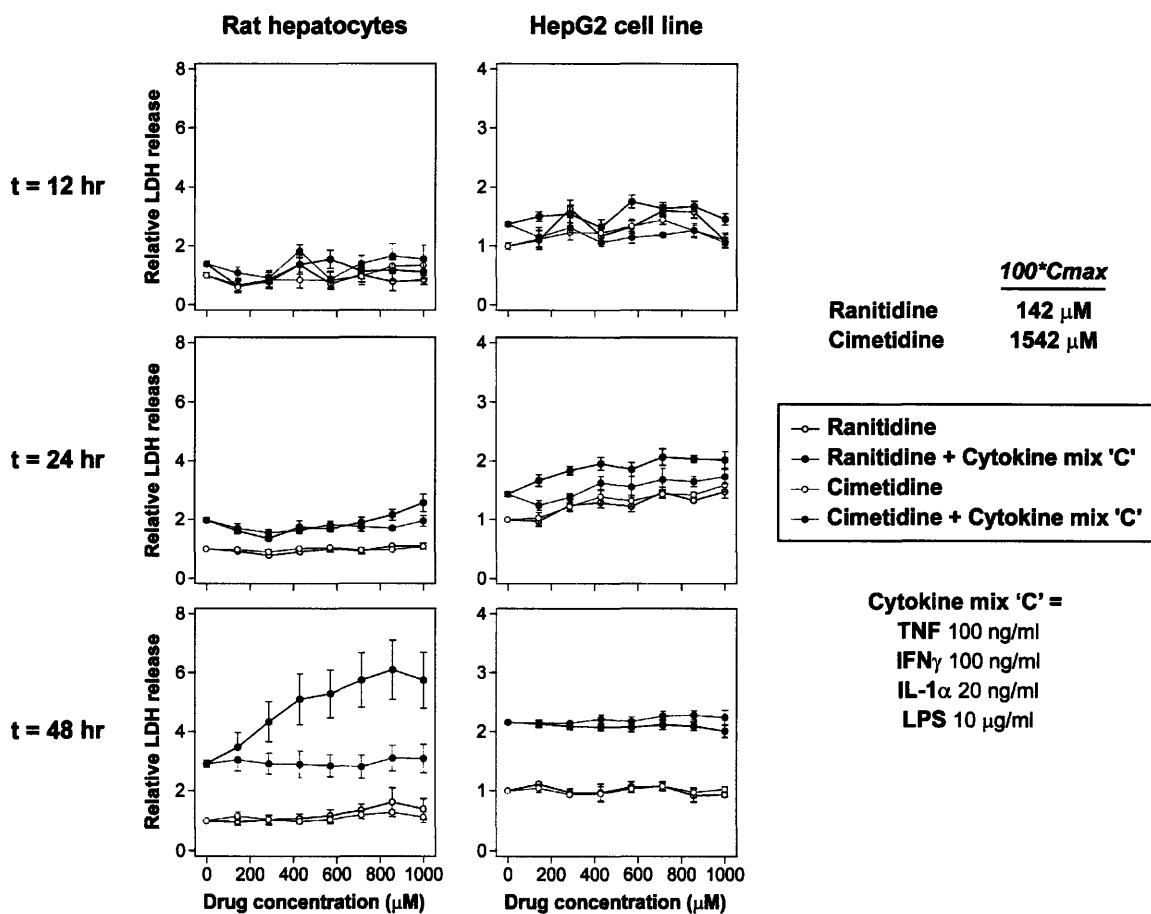


Figure 13. Dose-response curves of the ranitidine-cimetidine drug pair from the mean LDH release data in both cell systems at three time points. Ranitidine showed clear drug-cytokine synergy around 450 µM at 24 and 48 hours in primary rat hepatocytes. Error bars represent the standard error across four or more biological replicates.

Levofloxacin - Trovafloxacin

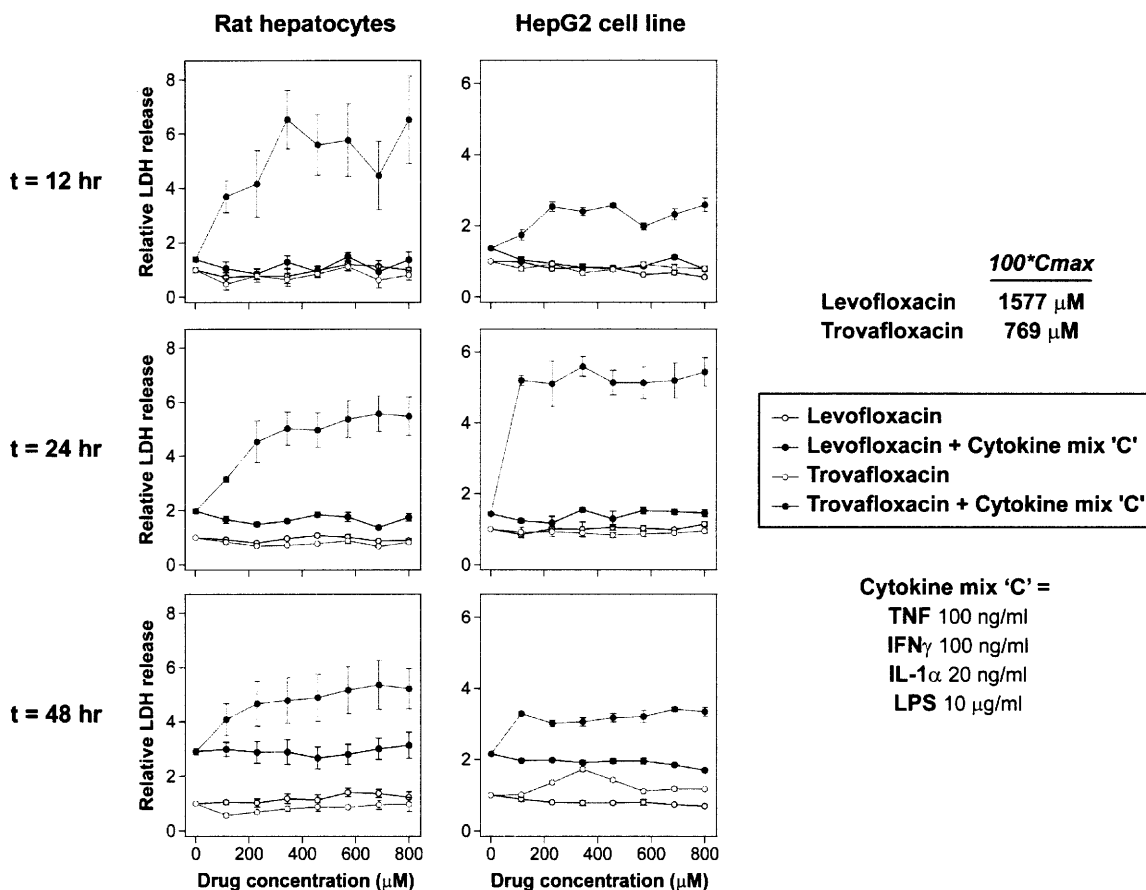


Figure 14. Dose-response curves of the levofloxacin-trovafloxacin drug pair from the mean LDH release data in both cell systems at three time points. Trovafloxacin showed clear drug-cytokine synergy around 450 μ M at 24 and 48 hours in HepG2s and primary rat hepatocytes. Error bars represent the standard error across four or more biological replicates.

Entacapone - Tolcapone

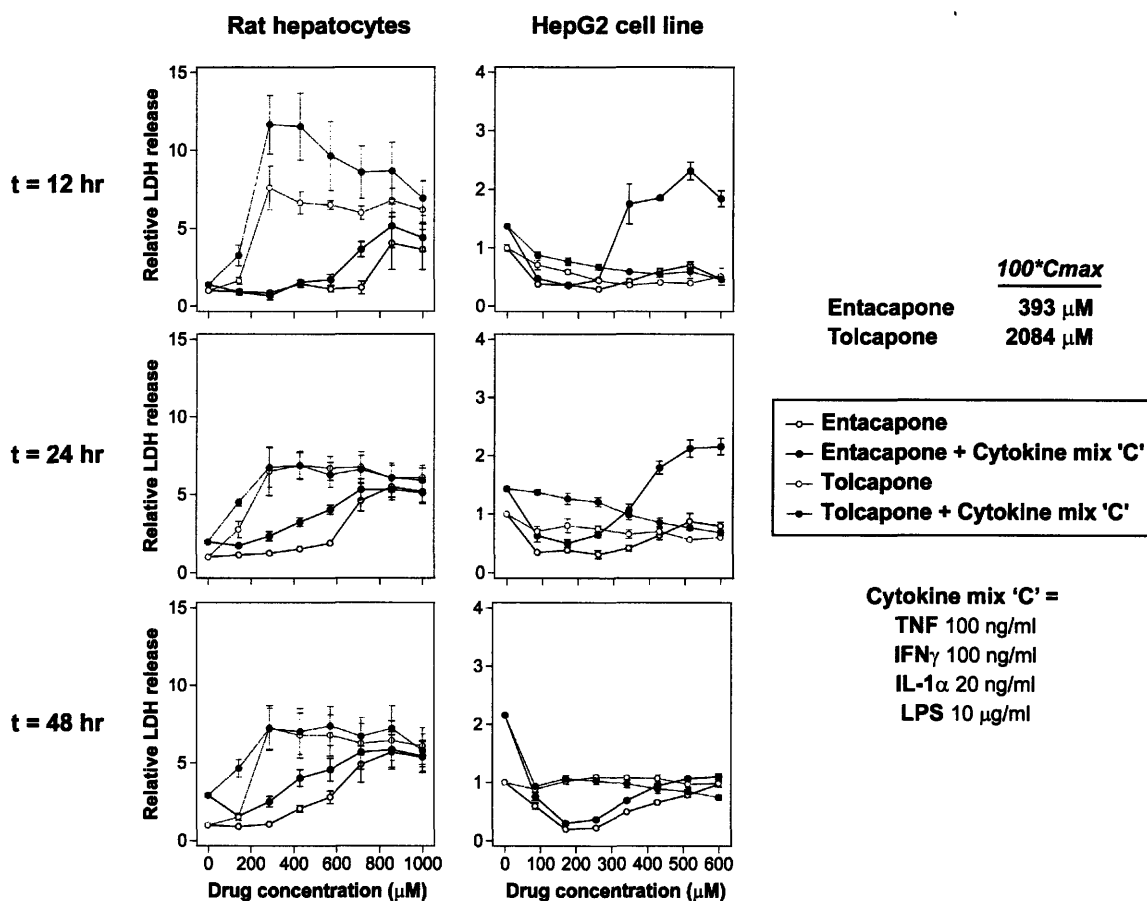


Figure 15. Dose-response curves of the entacapone-tolcapone drug pair from the mean LDH release data in both cell systems at three time points. Neither drug showed clear drug-cytokine synergy at any time point in either cell system. Error bars represent the standard error across four or more biological replicates.

4.3 Drug-cytokine synergy calculations

As explained in Section 2.3.5, we then set about to qualitatively identify a single drug concentration that demonstrated synergistic toxicity in both cell systems for each compound. A representative graph is shown below (Figure 16), with the concentration listed from the experiment in which the projected toxicity value most under-predicted that obtained experimentally. These results are compiled in Table 4. Table 5 presents the drugs and their corresponding concentrations that were selected for the 5-cytokine/LPS multiplex experiments.

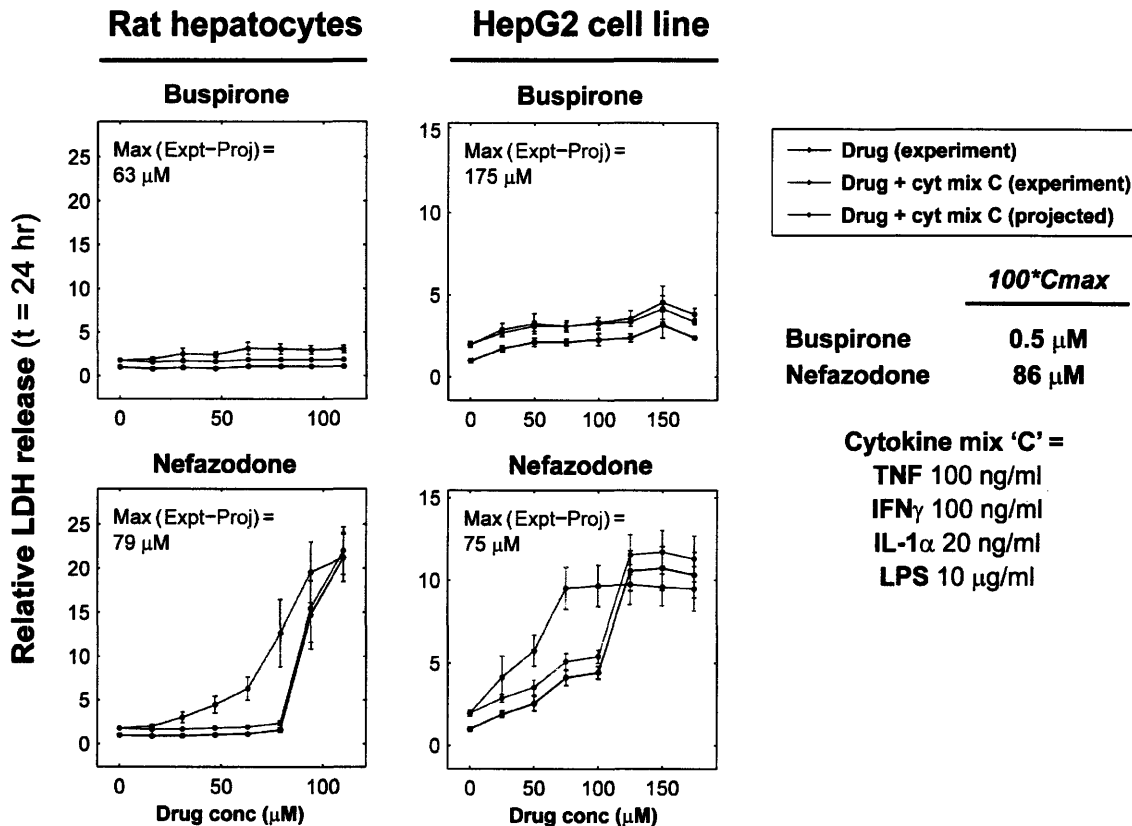


Figure 16. Measured dose-response curves for the buspirone-nefazodone drug pair compared to those predicted by the additive cytotoxicities of drug and an inflammatory cytokine background. Data is presented from the mean LDH release data set in both cell systems at 24 hours. Error bars represent the standard error across four or more biological replicates.

Table 4. Calculated drug concentrations displaying the maximum drug-cytokine synergy in both cell systems at three time points, according to the LDH release data set. The time points in each cell system at which synergy was observed (Table 5) are shown in red.

Drug	Concentration of max synergy (μM)					
	Rat hepatocytes			HepG2s		
	12hr	24hr	48hr	12hr	24hr	48hr
Buspirone	94	63	110	175	175	-
Nefazodone	110	79	79	125	75	-
Clarithromycin	429	286	286	364	243	61
Telithromycin	357	357	357	121	121	121
Aspirin	857	857	1000	750	643	-
Nimesulide	1000	857	857	750	429	214
Ranitidine	571	1000	857	571	857	857
Cimetidine	429	-	1000	-	-	857
Levofloxacin	343	-	114	686	343	229
Trovafloxacin	343	686	686	457	343	114
Entacapone	714	571	429	514	600	-
Tolcapone	429	143	143	-	86	-

Table 5. Drugs selected for testing in the 5-cytokine/LPS multiplex experiment. The concentration used in subsequent experiments is shown for a given drug, as well as the cell system and time point in which synergy was previously observed.

Drugs selection for drug-cytokine combinatorial experiments

Drug	Concentration (μM , vs C_{max})	End point	Synergy with cytokine mix in...		Synergy in LPS-administered animal model (Roth group)
			Rat hep's	HepG2 cells	
Nefazodone	75 μM = 78* C_{max}	24 hr	+	+	<i>not reported</i>
Clarithromycin	175 μM = 52* C_{max}	24, 48 hr	+	+	<i>not reported</i>
Telithromycin	175 μM = 63* C_{max}	24, 48 hr	-	-	<i>not reported</i>
Nimesulide	450 μM = 21* C_{max}	24 hr	-	+	<i>not reported</i>
Ranitidine	450 μM = 317* C_{max}	24, 48 hr	+	-	+
Trovafloxacin	450 μM = 59* C_{max}	24 hr	+	+	+

Color key: *Compound not associated with liver injury*

Compound associated with idiosyncratic liver injury (DILI P2)

5 5-cytokine/LPS multiplexing

5.1 Results from human hepatoma cell line

The most prominent trend evident from both the caspase 3/7 activity and LDH release assays was the overwhelmingly synergistic effect of TNF across multiple drug backgrounds (Figure 17). Even by inspection, TNF was clearly shown to play a role in determining hepatotoxicity in the HepG2 cell line (Figures A3, A5). This was especially true in the cases of clarithromycin, nefazodone, trovafloxacin, and nimesulide. Interestingly, TNF was calculated to have a significant main effect on caspase 3/7 activity assay values across all backgrounds at both time points (Figure A4). These effects dominated other effects and interactions in the cases of all four drug backgrounds previously mentioned. In the cases of DMSO and ranitidine backgrounds at both 24 and 48 hours, IFN γ was also calculated to have a significant effect. However, as explained in Section 2.3.1, these single effects cannot be interpreted because of their inclusion in the significant two-factor interaction TNF \times IFN γ . This two-factor interaction was also significant in the presence of clarithromycin, as was the negative interaction between TNF and IL-1 α . This significant negative TNF \times IL-1 α interaction was seen in the presence of nefazodone and trovafloxacin as well. Over a background of nefazodone, IFN γ showed a significant main effect at 24 hours in the HepG2s, as did IL-1 α .

Factorial effects calculated from the LDH release assay also identified TNF as having the most prominent effect among the cytokine/LPS combinations across the data set, again especially in the cases of clarithromycin, nefazodone, trovafloxacin, and nimesulide (Figure A6). This assay measured some of the same factorial trends that were mentioned earlier from the caspase 3/7 activity assay data, but they were not significant.

As would be expected, measured toxicities were generally greater at 48 than 24 hours (Figures A3, A5). Also, the relatively high toxicity levels measured by caspase 3/7 activity in the presence of TNF and IFN γ over a background of clarithromycin were not picked up by the LDH release assay (Figure 17).

5.2 Results from primary rat hepatocytes

Similar to the HepG2s, many of the TNF main effects were calculated to be statistically significant from caspase 3/7 activity data (Figure A8). In fact, the drug backgrounds for which the effect of TNF was statistically significant are the same that were prominent by the same assay at the same time point in the human hepatoma data set (Figures A4, A8), although by inspection only clarithromycin and trovafloxacin data sets exhibited this trend at 24 hours (Figure A7). A statistically significant two-factor interaction between IL-1 α and IL-6 was measured over a DMSO background by the caspase 3/7 activity assay at 24 hours (Figure A8), as well as by both assays at 48 hours (Figures A8, A10). As before, this means that the significant effect of IL-1 α at 48 hours as measured by the LDH release assay cannot be individually interpreted (Figure A10). Additionally, a consistent TNF \times IL-1 α interaction was clear at both time points in the primary rat hepatocytes in the presence of clarithromycin (Figures A8, A10). Those LDH release assay values measured at 24 hours were also overwhelmed by the high toxicity values that were measured in the presence of nimesulide across the range of treatment conditions; the fold change scale measured for this data set was two to three times that measured for any of the other assay value heat maps presented in Figure 17. However, this data is consistent with that from the primary rat hepatocytes in Figure 12. In the same way, the corresponding heat map of factorial effects calculated from LDH release assay

data at 24 hours (Figure 17) was overwhelmed by the prominent main effect of TNF that was measured in the presence of trovafloxacin (Figure A10).

5.3 General trends across the data set

It must be noted that LPS was calculated to have significant effects in only three backgrounds across this data set and that none of them were very prominent (Figures A4, A8, A10). In addition, the prominent TNF \times IL-1 α interaction noted in HepG2s was also present in the primary rat hepatocytes. TNF and IFN γ seemed to independently have significant effects on toxicity in both cell systems, as measured by both assays at 24 and 48 hours (Figure 17). Toxicity increased noticeably across the range of treatment conditions by 48 hours as well.

5.4 Further analysis

The HepG2 data from 24 hours as measured by the caspase 3/7 activity assay was subsequently analyzed using a joint entropy estimation to identify those subsets of particularly informative cytokine treatments (Figure 18). Subsets of cytokine treatments were evaluated with as few as four and as many as 32 cytokine treatment conditions. Many unique cytokine treatments that were among the most representative subset of five treatments were also among the most representative subset of 15 treatments (e.g. TNF+LPS and TNF+IL-6+LPS). The cytokine combination of TNF and IL-6 most commonly appeared as a member of the informative subset, and cytokine mix C was a member of the most representative 4-treatment subset and the most representative 10-treatment subset, as well as a member of more populated subsets (Figure 18). In Figure 19, the entropies of these subsets that were optimized to contain the maximum amount of outcome information (best) are plotted versus the entropies of subsets that would have been chosen at random among the estimated 1000 subsets (average). Note that maximum joint entropy was reached by a 15-treatment set, indicating that more complicated treatment sets do not contain any more net residual information about drug-cytokine toxicity synergies. Also note that 90% of the total joint entropy was captured in the 10-treatment set.

Euclidean clustering of the caspase 3/7 activity data set from the HepG2 cell line at 24 hours qualitatively confirmed many of general trends that were observed by inspection (Figure 20). Data from the DMSO control, ranitidine, and telithromycin backgrounds clustered together as the least cytotoxic data sets. This was expected of both drugs since they previously displayed minimal drug-cytokine synergy in the human hepatoma cell

line (Table 5). As we have seen previously, increasing toxicity was generally associated with higher-order cytokine combinations (Figure 20). In particular, the presence of TNF in a given cytokine mix was the most significant determinant of treatment clustering, followed by either IFN γ or IL-1 α . The most informative cytokine treatment conditions chosen in the 10-treatment joint entropy evaluation are distributed into many clusters rather than into a few high toxicity clusters, illustrating the ability of joint entropy analysis to identify a treatment subset that exhibits a diverse set of toxicity outcomes.

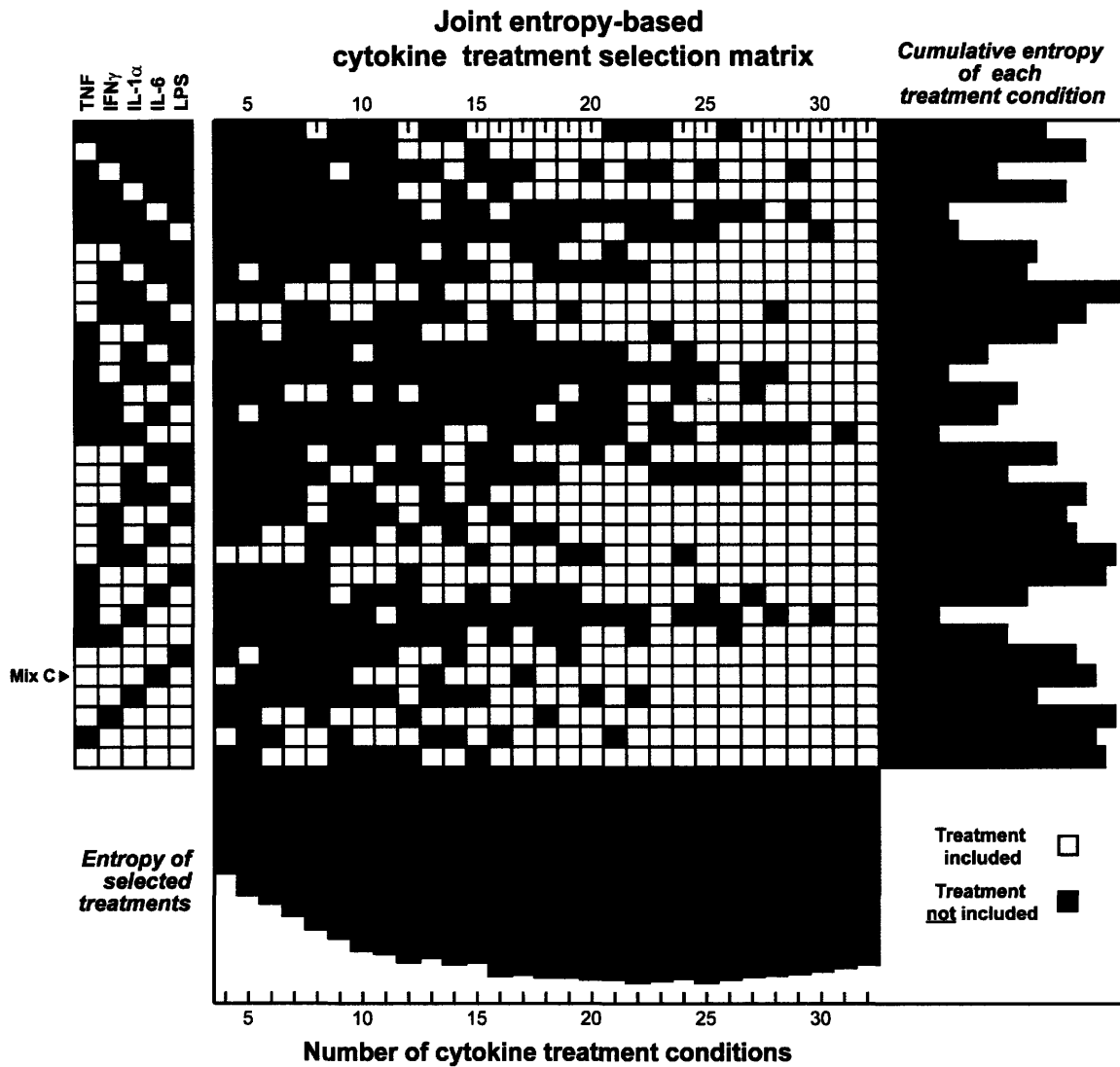


Figure 18. Selection matrix to choose the most representative set of cytokine treatments, given a specific number of possible cytokine conditions. The subset of the highest calculated joint entropy was chosen. Entropies of selected treatment sets (bottom) and accumulated for each treatment condition (right) are plotted in red [Bracken King].

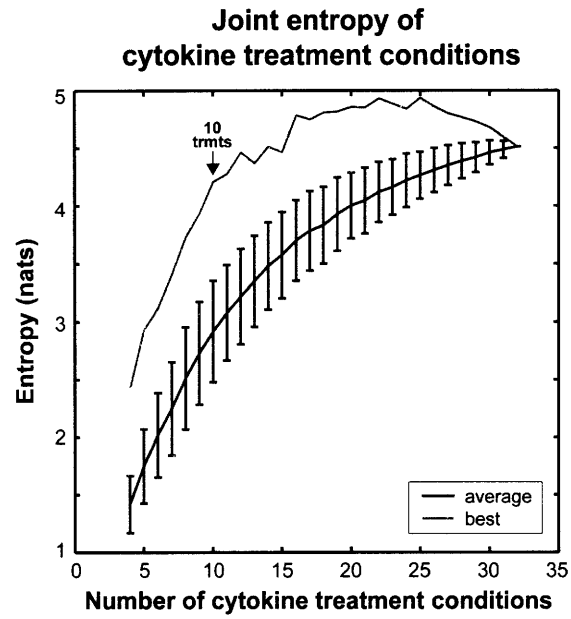


Figure 19. Comparison of the information content described by an average subset of treatments versus the best (most informative) treatment set as identified in Figure 18, given a specific number of conditions [Bracken King].

HepG2 cell line, Caspase 3/7 activity
t = 24 hr

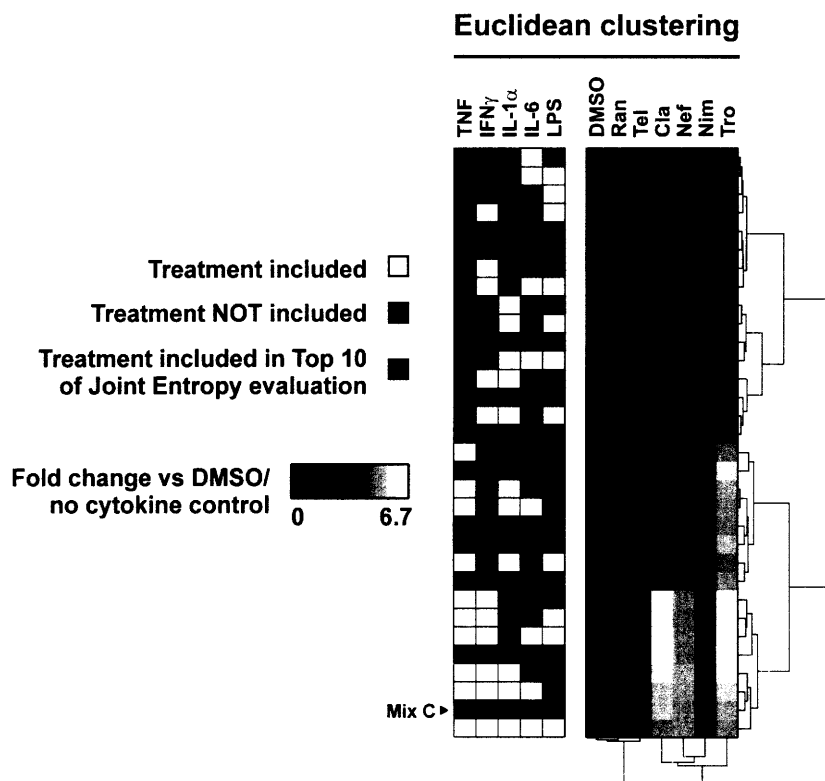


Figure 20. Euclidean clustering of the caspase 3/7 activity data set from the HepG2 human hepatoma cell line at 24 hours. TNF, followed by either IFN γ or IL-1 α , were major determinants of treatment clustering. Those ten treatments that were identified by the joint entropy-based evaluation to best predict the outcomes in this data set are noted.

5.5 Conclusions

It is interesting that TNF figured so prominently in the factorial effects calculated for both the HepG2s and primary rat hepatocytes. As shown in Figure 21, its signal is transduced upon receptor binding via the I κ B, JNK, and p38 MAPK pathways. It is important, however, to keep in mind that the significant factorial contribution of TNF does not imply that TNF is the most informative or representative of the cytokines in predicting toxicity outcomes. In fact, TNF does not appear alone in the joint entropy-based treatment selection matrix until a subset of 12 conditions is considered (Figure 18). Moreover, the *absence* of cytokines appears in a subset before the first cytokine-alone condition is included (IFN γ), and no cytokine-only treatments are included in the Top 10.

Rather, this factorial data should be interpreted to mean that the presence of TNF in a given treatment mix generally increases its toxicity, and this increase is sometimes irrespective of the presence or absence of other cytokines/LPS. Also, it may be inferred that significant negative two-order interactions, in which the two cytokines/LPS also have significant positive main effects, result from signaling pathways being overwhelmed in the presence of both cytokines/LPS.

Variations across the data set as measured by caspase 3/7 activity and LDH release assays may result from differences in the mechanism of cell death, in the cell systems themselves, or both. For example, the toxicity measured in HepG2s in the presence of TNF and IFN γ over a clarithromycin background by caspase 3/7 activity was relatively greater than that measured by the LDH release assay (Figure 17). Potentially, this could be explained by the presence of apoptotic cells, which had not yet undergone secondary necrosis. Furthermore, it is encouraging that the results compiled in Table 5 are repeated in Figure 17; nimesulide and ranitidine only showed synergistic toxicity in the HepG2 cell line and primary rat hepatocytes, respectively.

6 Discussion

Having established a systematic multiplexing approach, we developed an *in vitro* system to study and model cytokine-mediated idiosyncratic drug hepatotoxicity, recapitulating the *in vivo* situation. It is promising that some of the treatment-outcomes we observed clearly demonstrated the same phenotypes as those seen by Roth's group. In our model, unique inflammatory cytokine stimulation caused cell system-specific hepatotoxicity, which may be extended in the future to include animal model- or patient-specific toxicity as well. We consistently saw synergistic toxicity in the presence of multiple idiosyncratic drugs across a landscape of inflammatory backgrounds. It would be interesting to obtain data showing animal-to-animal or patient-to-patient variability in cytokine upregulation following LPS administration or other inflammatory stimulation to support our hypothesis that unique cytokine backgrounds mediate drug toxicity outcomes. In fairness, however, it must also be mentioned that many of the cases of idiosyncratic drug hepatotoxicity *in vivo* occurred in patients with chronic - versus acute - inflammation, a condition that has not been extensively examined in our *in vitro* systems. Additionally, some of the drugs we tested might interfere with one or more of our lethal endpoint assays due to enzyme inhibition; in particular, we hypothesize that this may be the case for telithromycin and trovafloxacin. In the future, we intend to investigate and potentially correct for these interactions, while following up on this study by testing for synergistic toxicity between the Top 10 cytokine/LPS combinations and multiple drugs in primary hepatocytes and by further querying mechanisms of hepatotoxicity via cell imaging and intracellular signaling platforms. This model may one day be used to

identify diagnostic biomarkers that predict the effects of treatments and interventions for therapeutic applications.

7 Future Work

7.1 Primary human hepatocytes

We hope to compare our data from HepG2s and primary rat hepatocytes to that from cryo-preserved primary human cellular systems (CellzDirect) to investigate the similarities and differences in their responses to drug administration, given an induced inflammatory environment. The ten or so cytokine/LPS combinations identified to be the most informative by joint entropy calculations and shown to exhibit a range of toxicities will be co-administered with drugs to effectively cover a landscape of phenotypic responses and cell signaling pathways.

7.2 Cellomics imaging

In the future we also hope to measure the responses of various cell systems using the Cellomics platform at Pfizer's Research Technology Center in Cambridge, MA. This high-throughput imager assesses nuclei, lipid, and glutathione content, as well as bile canaliculi function, mitochondrial membrane potential, and reactive oxygen species, of single cells. Measurements of these sub-lethal toxicities may provide more information regarding the mechanisms of hepatotoxicity.

7.3 Intracellular signaling

A systems-level approach is necessary to quantify the complex signal transduction between environmental cues and intracellular signals that define disease states, building a landscape of "toxicity-associated" signaling and hopefully elucidating mechanisms of hepatocarcinogenesis. The high-throughput, quantitative multiplex Bio-Plex technology from Bio-Rad Laboratories in Hercules, CA, utilizes multiplex bead-based assays to evaluate the phosphorylation states within particular pathways of signaling proteins.

Sampling phosphoprotein levels at critical nodes within this network will quantitatively monitor information flow regarding hepatocyte injury. Identifying relevant kinases, such as Akt (Ser⁴⁷³), ERK1/2 (Thr²⁰²/Tyr²⁰⁴, Thr¹⁸⁵/Tyr¹⁸⁷), GSK-3 α / β (Ser²¹/Ser⁹), I κ B- α (Ser³²/Ser³⁶), JNK (Thr¹⁸³/Tyr¹⁸⁵), p38 MAPK (Thr¹⁸⁰/Tyr¹⁸²), STAT3 (Tyr⁷⁰⁵), HSP27 (Ser⁷⁸), IRS-1 (Ser⁶³⁶/Ser⁶³⁹), MEK1 (Ser²¹⁷/Ser²²¹), p53 (Ser¹⁵), Histone H3 (Ser¹⁰), and p70 S6 kinase (Thr⁴²¹/Ser⁴²⁴), in the idiosyncratic drug hepatotoxicity pathway and monitoring their levels with respect to time will help construct quantitative, dynamic, predictive models of cue-signal-phenotypic response relationships that include key nodes in all the major pathways. In this model of cytokine-induced hepatotoxicity, idiosyncratic and non-idiosyncratic drugs will be co-administered to susceptible cytokine/LPS-stimulated hepatocytes, and kinase phosphorylation will be monitored with time to provide insight into the state of the signaling network. For the purposes of the PLSR statistical model, we plan to focus on the ten or so cytokine treatments that were identified using joint entropy evaluations to collect an intracellular signaling time course data set in the presence and absence of both idiosyncratic and non-idiosyncratic drugs. Preliminary experiments have already been performed to ensure Bio-Plex operation in a linear dynamic range. Cell lysis and antibody detection were performed per the manufacturer's recommendations and were analyzed using Luminex technology and Bio-Plex Manager software. We hope this research would, in conjunction with data on drug metabolism and the mechanism of drug toxicity, provide information regarding the cell decision process.

Hepatocyte Signaling Network

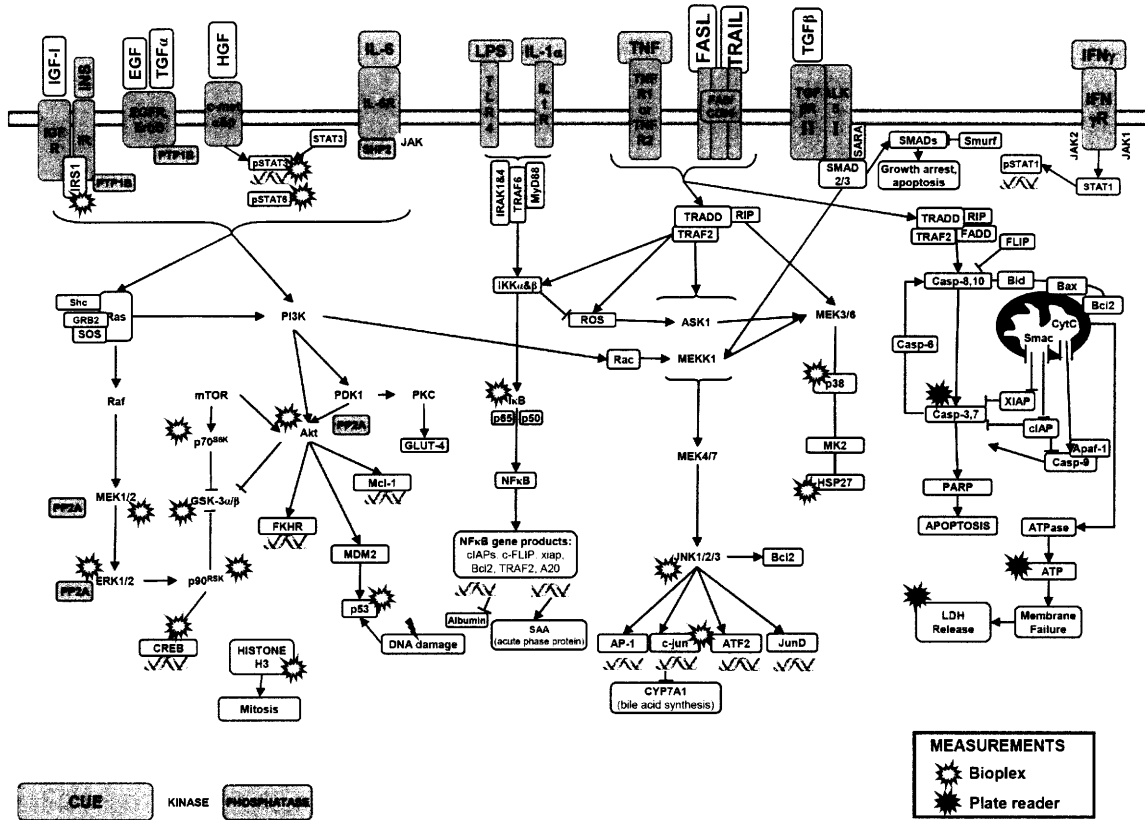


Figure 21. Intracellular signaling network of hepatocytes. All cues used in this study are identified, as well as some of the kinases whose phosphoprotein levels will be measured using the Bio-Plex platform in future work [adapted from Leonidas Alexopoulos].

8 References

- Adamson, G.M. and R.E. Billings [1993]. "Cytokine toxicity and induction of NO synthase activity in cultured mouse hepatocytes." Toxicology and Applied Pharmacology 119: 100-107.
- Barton, C.C., D.A. Hill, S.B. Yee, E.X. Barton, P.E. Ganey, and R.A. Roth [2000]. "Bacterial lipopolysaccharide exposure augments aflatoxin B(1)-induced liver injury." Toxicological Sciences 55: 444-452.
- Bergheim, I., J.P. Luyendyk, C. Steele, G.K. Russell, L. Guo, R.A. Roth, and G.E. Arteel [2006]. "Metformin prevent endotoxin-induced liver injury after partial hepatectomy." Journal of Pharmacology and Experimental Therapeutics 316: 1053-1061.
- Block, G.D., J. Locker, W.C. Bowen, B.E. Petersen, S. Katyal, S.C. Strom, T. Riley, T.A. Howard, and G.K. Michalopoulos [1996]. "Population Expansion, Clonal Growth, and Specific Differentiation Patterns in Primary Cultures of Hepatocytes Induced by HGF/SF, EGF and TGF α in a Chemically Defined (HGM) Medium." Journal of Cell Biology 132: 1133-1149.
- Box, G.E.P., W.G. Hunter, and J.S. Hunter [1978]. Statistics for Experimenters. New York, John Wiley & Sons.
- Brandonm E.F.A., C.D. Raap, I. Meijerman, J.H. Beijnen, and J.H.M. Schellens [2003]. "An update on in vitro test methods in human hepatic drug biotransformation research: pros and cons." Toxicology and Applied Pharmacology 189: 233-246.
- Cosgrove B.D., C Cheng, D.B. Stolz, D.A. Lauffenburger, and L.G. Griffith. "TNF-induced hepatocyte proliferation and apoptosis are both regulated by a coupled TGF- α -IL-1 α / β autocrine circuit." *in preparation*.
- D'haeseleer, P. [2005]. "How does gene expression clustering work?" Nature Biotechnology 23: 1499-1501.
- Geladi P., and B.R. Kowalski [1986]. "Partial least-squares regression: a tutorial." Analytica Chimica Acta 185: 1-17.
- Janes K.A., S. Gaudet, J.G. Albeck, U.B. Nielsen, D.A. Lauffenburger, P.K. Sorger [2006]. "The response of human epithelial cells to TNF involves an inducible autocrine cascade." Cell 124: 1225-1239.
- Kaplowitz, Neil [2005]. "Idiosyncratic Drug Hepatotoxicity." Nature Reviews 4: 489-499.
- King, B.M. and B. Tidor. "High-order entropy approximation for dimension reduction of biological data sets." *in preparation*.
- Luedde, T. and C. Trautwein [2006]. "Intracellular survival pathways in the liver." Liver International 26: 1163-1174.
- Luyendyk, J.P., L.D. Lehman-McKeeman, D.M. Nelson, V.M. Bhaskaran, T.P. Reilly, B.D. Car, G.H. Cantor, J.F. Maddox, P.E. Ganey, and R.A. Roth [2006]. "Unique Gene Expression and Hepatocellular Injury in the Lipopolysaccharide-Ranitidine Drug Idiosyncrasy Rat Model: Comparison with Famotidine." Toxicological Sciences 90: 569-585.
- Miller-Jensen, K., K.A. Janes, J.S. Brugge, and D.A. Lauffenburger [2007]. "Common effector processing mediates cell-specific responses to stimuli." Nature 448: 604-608.

- Shults, M.D., K.A. Janes, D.A. Lauffenburger, and B. Imperiali [2005]. "A multiplexed homogeneous fluorescence-based assay for protein kinase activity in cell lysates." Nature Methods 2: 1-7.
- Sivaraman A., J.K. Leach, S. Townsend, T. Iida, B.J. Hogan, D.B. Stolz, R. Fry, L.D. Samson, S.R. Tannenbaum, and L.G. Griffith [2005]. "A microscale in vitro physiological model of the liver: predictive screens for drug metabolism and enzyme induction." Current Drug Metabolism 6: 569-91.
- Tukov, F.F., J.F. Maddox, D.E. Amacher, W.F. Bobrowski, R.A. Roth, and P.E. Ganey [2006]. "Modeling inflammation-drug interactions in vitro: a rat Kupffer cell-hepatocyte coculture system." Toxicology in vitro 20: 1488-1499.
- Waring, J.F., M.J. Liguori, J.P. Luyendyk, J.F. Maddox, P.E. Ganey, R.F. Stachlewitz, C. North, E.A.G. Blomme, and R.A. Roth [2006]. "Microarray Analysis of Lipopolysaccharide Potentiation of Trovafloxacin-Induced Liver Injury in Rats Suggests a Role for Proinflammatory Chemokines and Neutrophils." The Journal of Pharmacology and Experimental Therapeutics 316: 1080-1087.
- Xu, J.J., D. Diaz, and P.J. O'Brien [2004]. "Applications of cytotoxicity assays and pre-lethal mechanistic assays for assessment of human hepatotoxicity potential." Chemico-Biological Interactions 150: 115-128.
- Zhou, Z., Z. Song, J.J. Saari, C.J. McClain, and Y.J. Kang [2004]. "Abrogation of nuclear factor- κ B activation is involved in zinc inhibition of lipopolysaccharide-induced tumor necrosis factor- α production and liver injury." American Journal of Pathology 164: 1547-1556.

9 Appendices

9.1 Appendix 1. Hepatocyte growth medium recipe

Table A1. Recipe for hepatocyte growth medium, as added to 500 mL DMEM.

Supplement	Final Concentration
L-Proline	0.030 mg/mL
L-Ornithine	0.100 mg/mL
Niacinamide	0.305 mg/ml
D-(+)-Glucose	2.250 mg/ml
D-(+)-Galactose	2.000 mg/ml
BSA	2.000 mg/ml
ZnCl ₂	54.4 ng/ml
ZnSO ₄ ·7H ₂ O	75.0 ng/ml
CuSO ₄ ·5H ₂ O	20.0 ng/ml
MnSO ₄	25.0 ng/ml
L-Glutamine	1.0 mM
Sodium selenite	5.0 ng/ml
Trichostatin A	300 ng/ml
Insulin	5.0 ug/ml
Dexamethasone	0.1 uM
Gentamicin	0.10%
Transferrin	5.0 ug/ml

*DMEM has 1.0 mg/mL D-(+)-Glucose

9.2 Appendix 2. Primary rat hepatocyte data from 6-cytokine/LPS multiplex
Primary rat hepatocytes
Caspase 3/7 activity

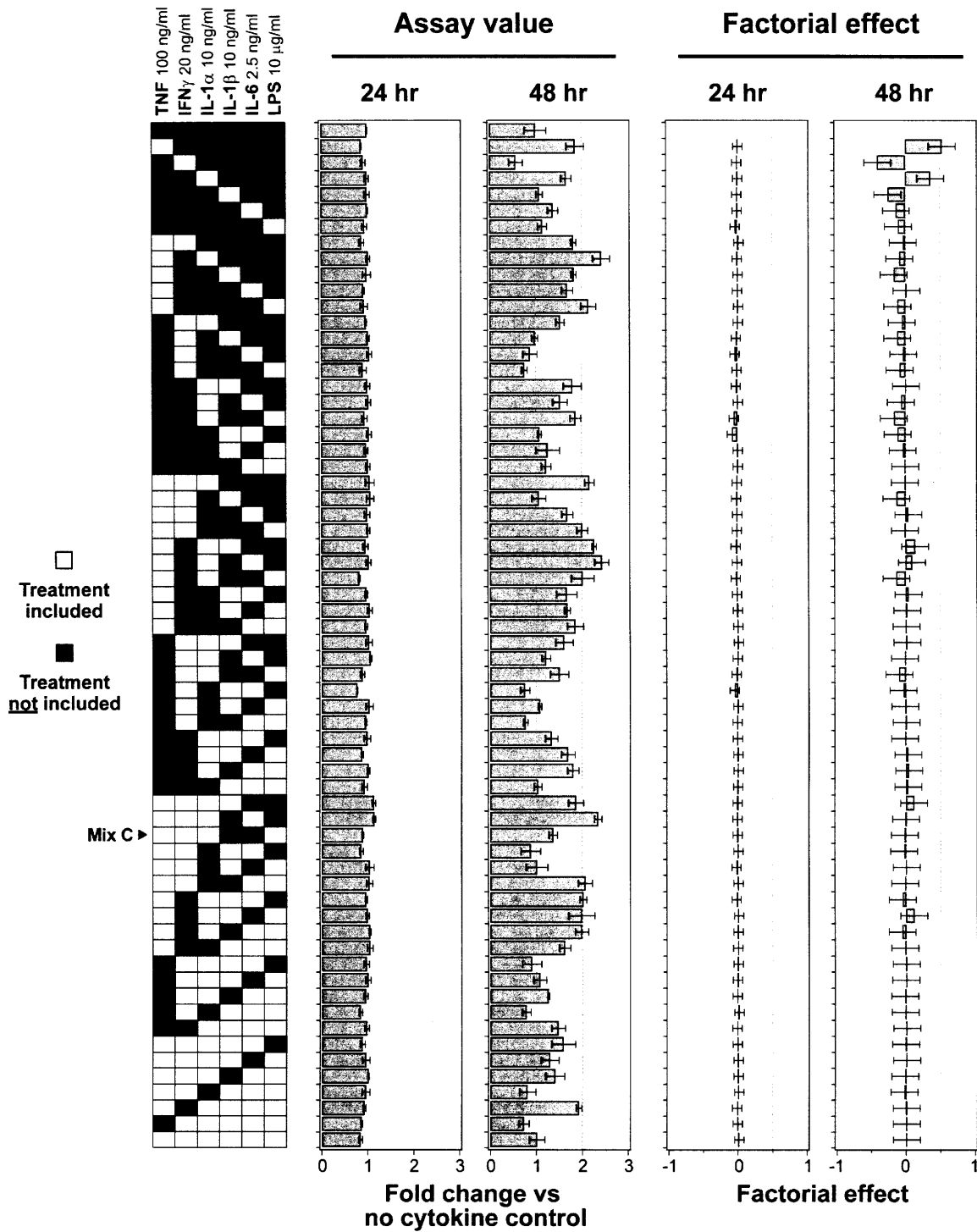


Figure A1. Mean caspase 3/7 activity assay values across the 64 treatment conditions and the factorial effects of those interactions in primary rat hepatocytes at two time points. Error bars in all graphs represent the standard error across three or more biological replicates.

Primary rat hepatocytes
LDH release

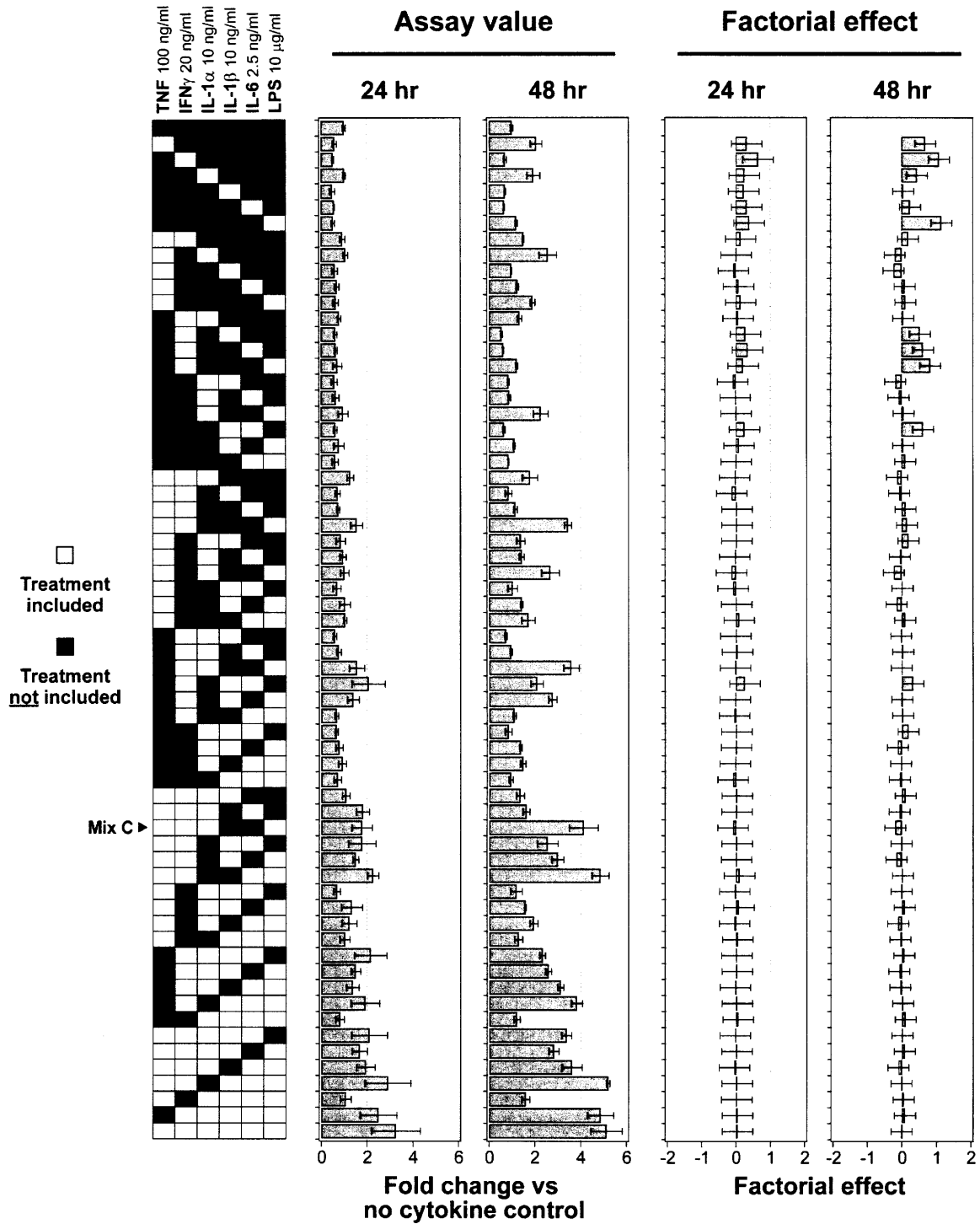


Figure A2. Mean LDH release assay values across the 64 treatment conditions and the factorial effects of those interactions in primary rat hepatocytes at two time points. Error bars in all graphs represent the standard error across three or more biological replicates.

9.3 Appendix 3. HepG2 data from 5-cytokine/LPS multiplex

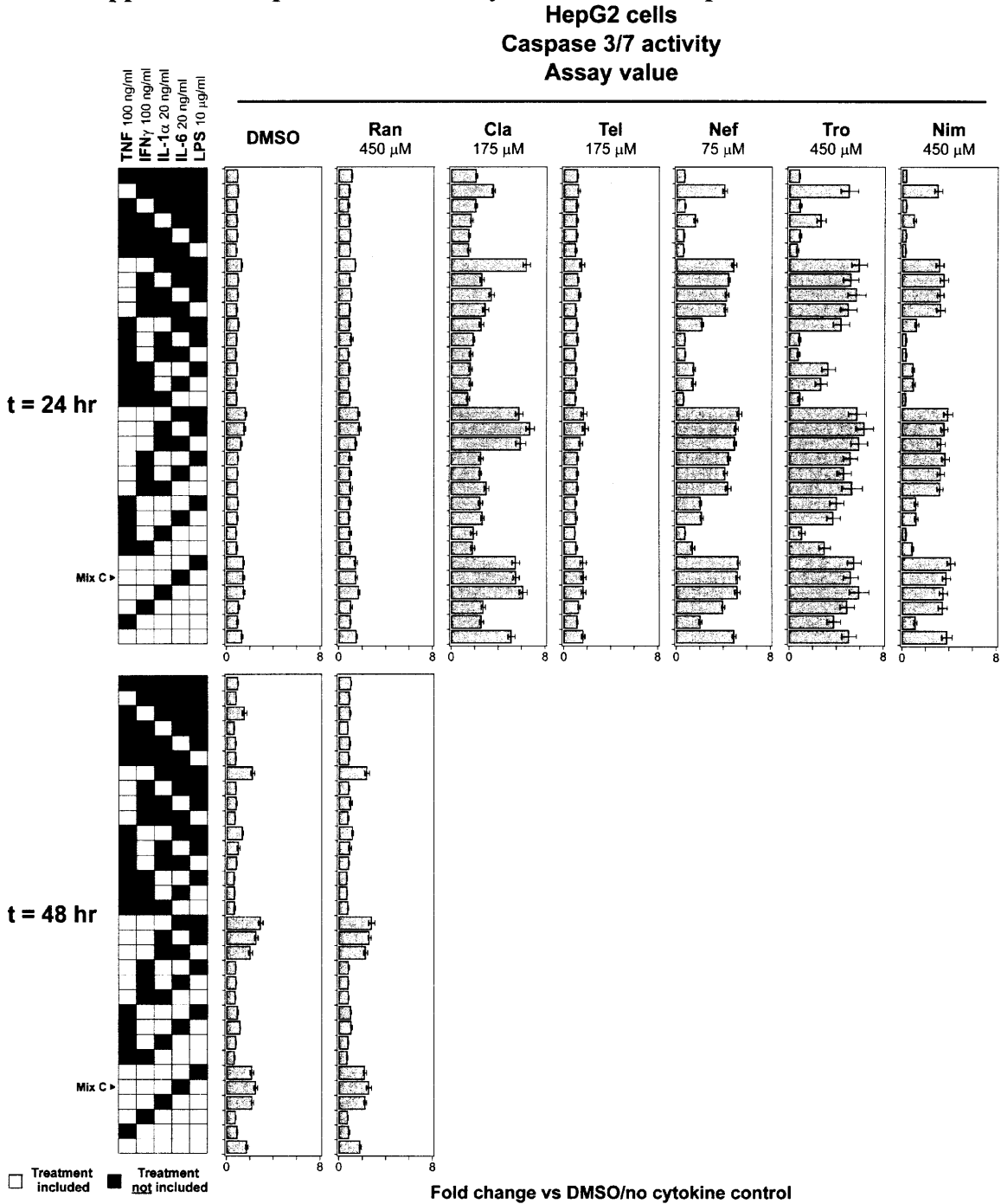


Figure A3. Mean caspase 3/7 activity assay values for HepG2s at two time points in the presence of six drugs. Error bars represent the standard error across five or more biological replicates.

HepG2 cells
Caspase 3/7 activity
Factorial effect

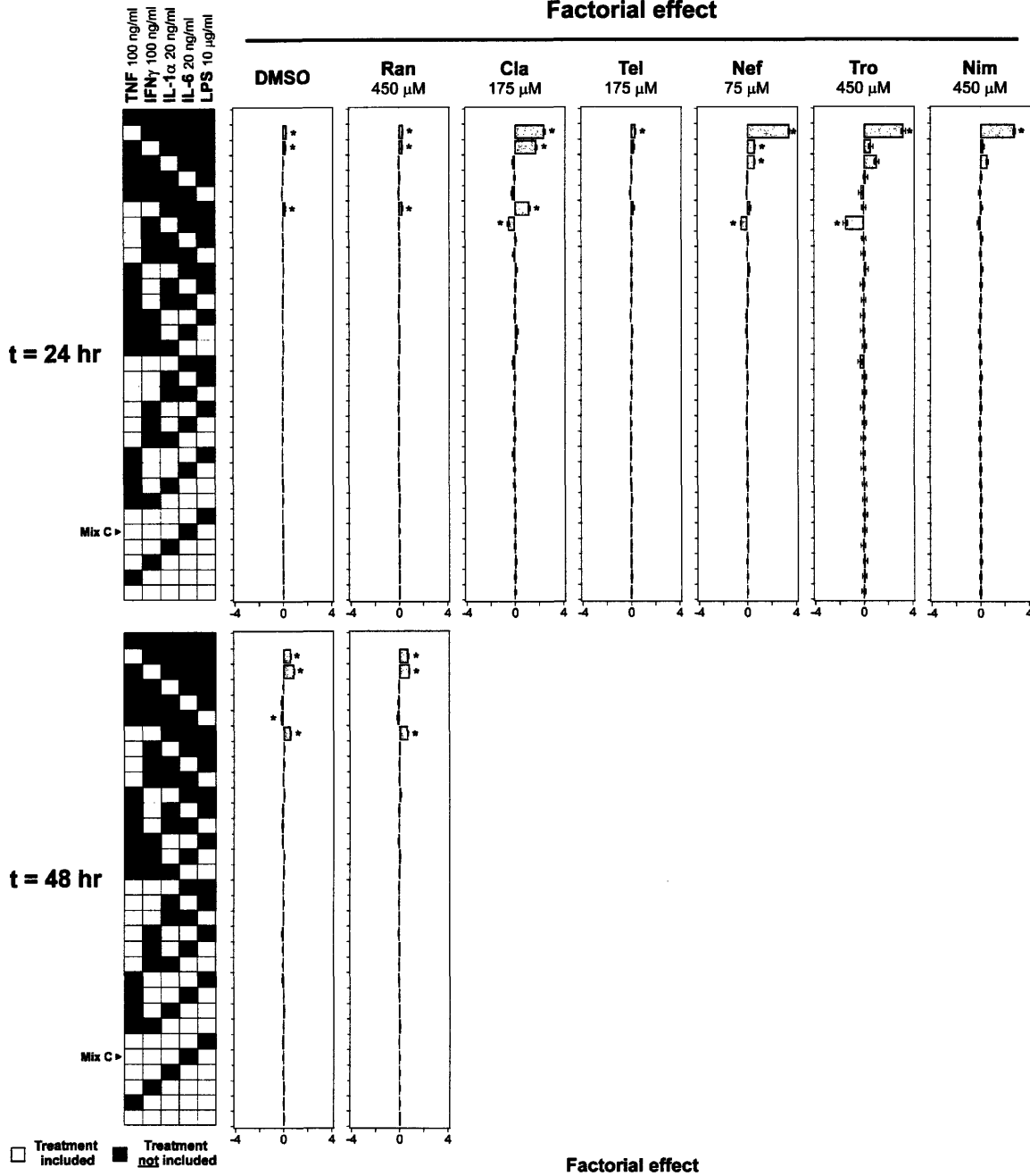


Figure A4. Mean factorial effects calculated from caspase 3/7 activity assay values for HepG2s at two time points in the presence of six drugs. Error bars represent the standard error across five or more biological replicates, and * denotes statistical significance.

HepG2 cells
LDH release
Assay value

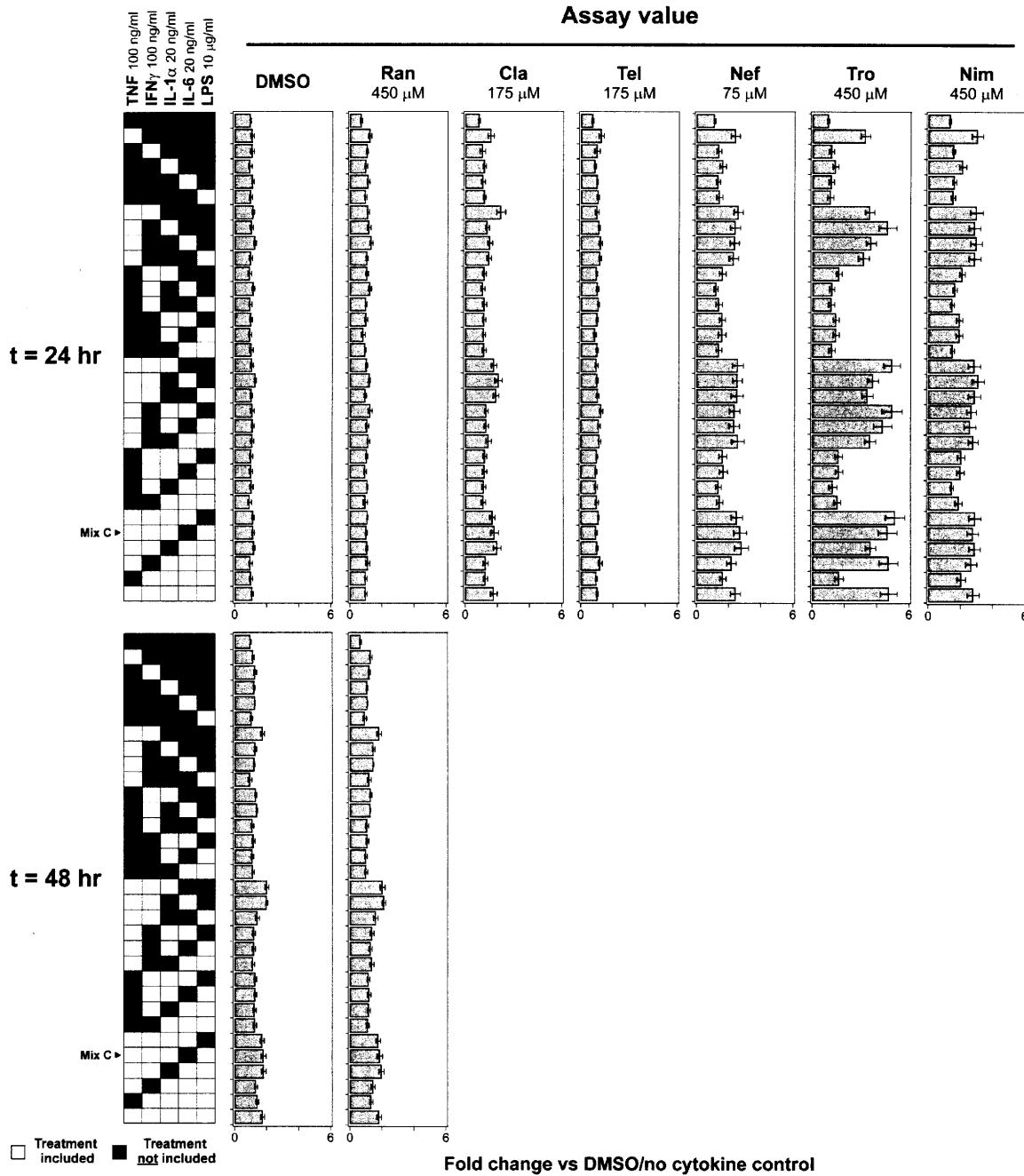


Figure A5. Mean LDH release assay values for HepG2s at two time points in the presence of six drugs. Error bars represent the standard error across five or more biological replicates.

HepG2 cells
LDH release
Factorial effect

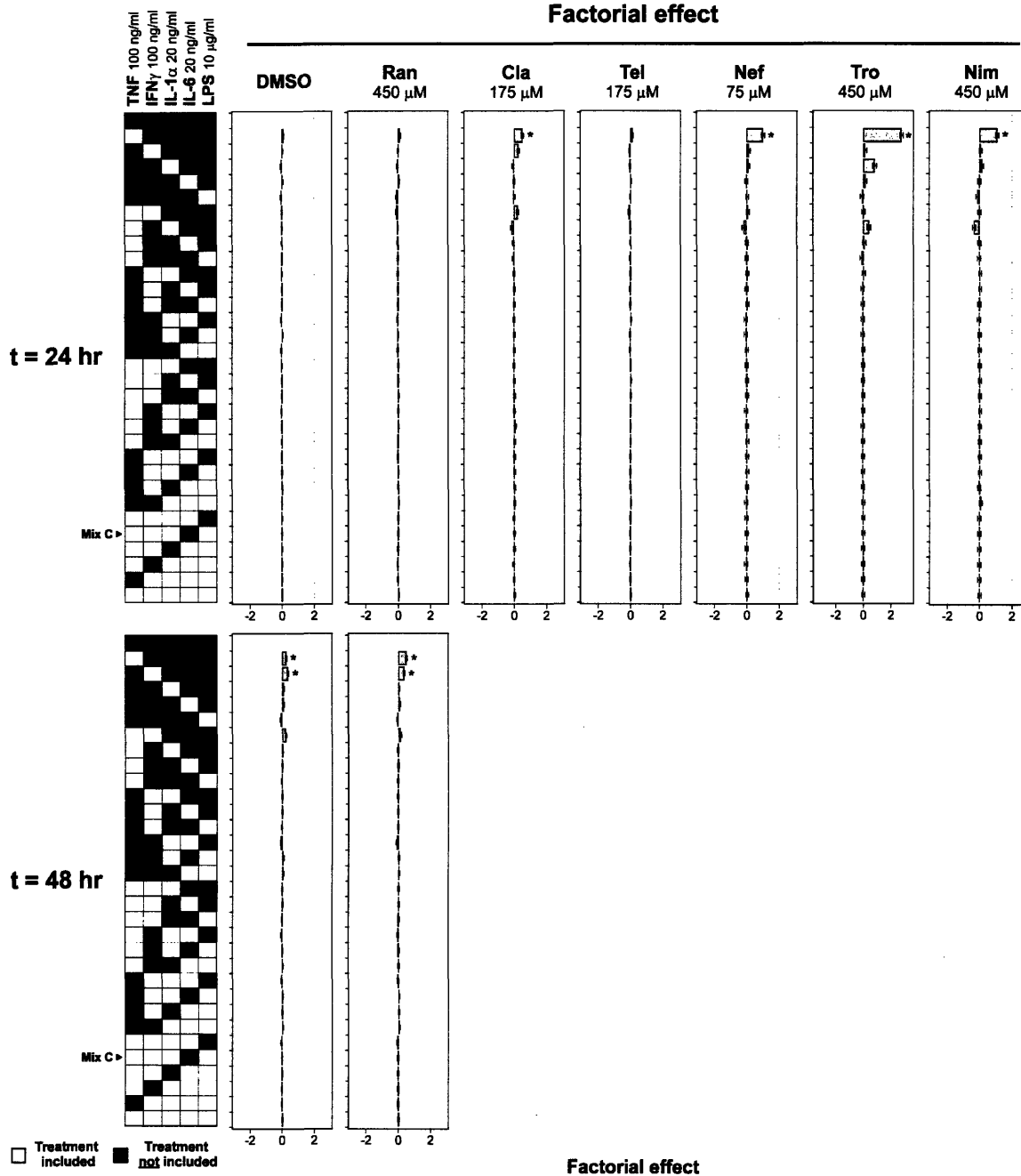


Figure A6. Mean factorial effects calculated from LDH release assay values for HepG2s at two time points in the presence of six drugs. Error bars represent the standard error across five or more biological replicates, and * denotes statistical significance.

9.4 Appendix 4. Primary rat hepatocyte data from 5-cytokine/LPS multiplex
 Primary rat hepatocytes
 Caspase 3/7 activity
 Assay value

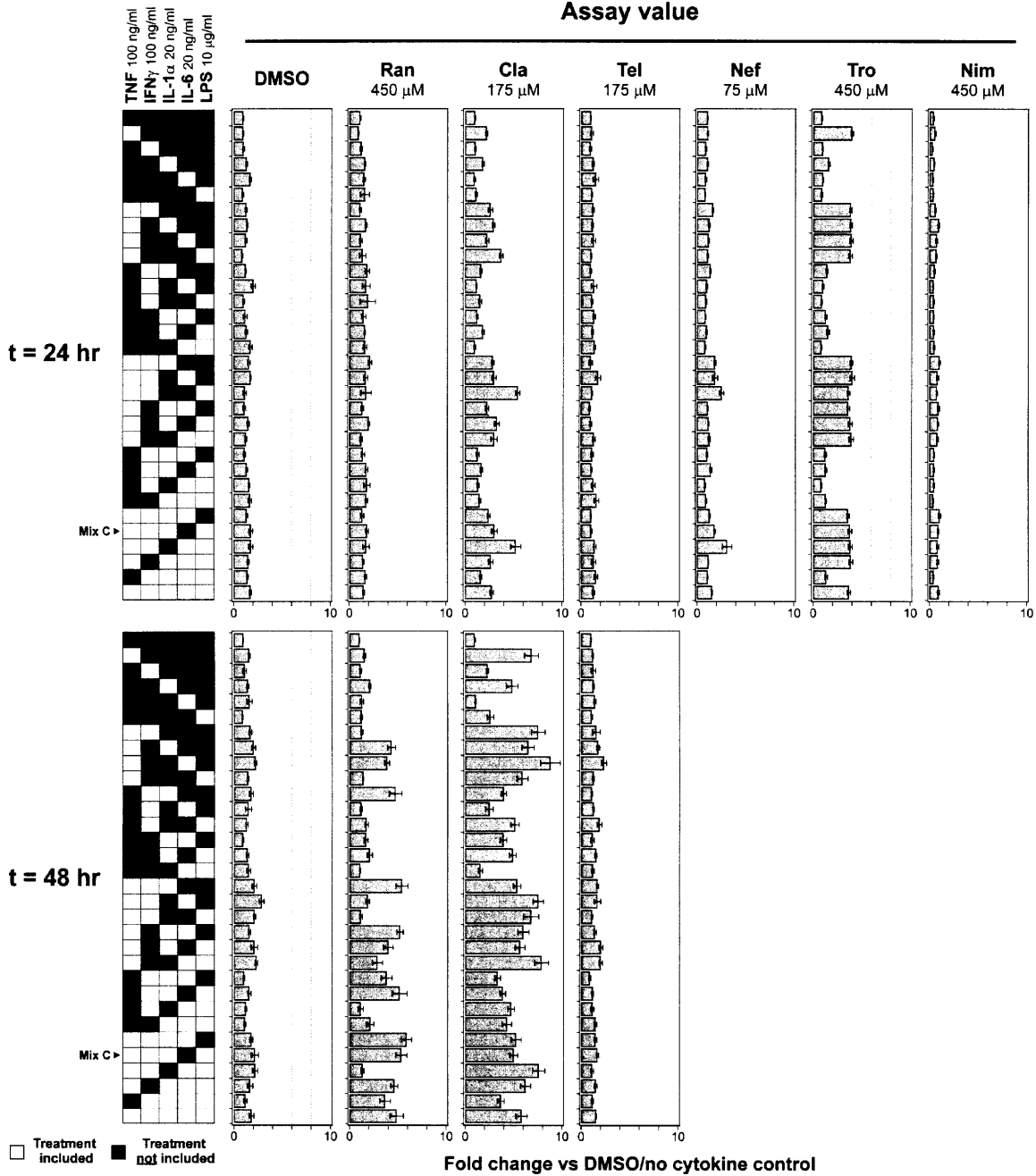


Figure A7. Mean caspase 3/7 activity assay values for primary rat hepatocytes at two time points in the presence of six drugs. Error bars represent the standard error across five or more biological replicates.

Primary rat hepatocytes
Caspase 3/7 activity
Factorial effect

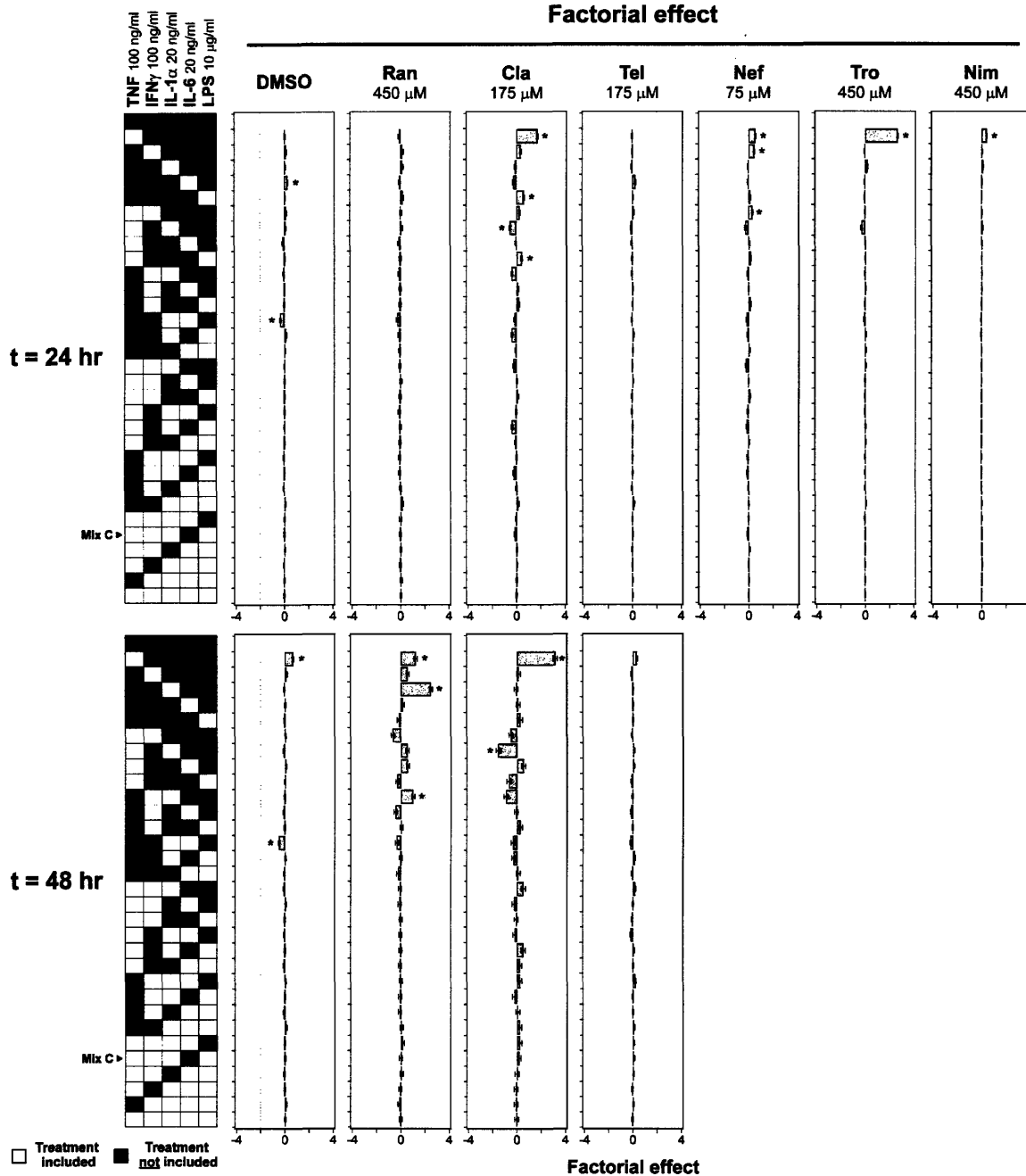


Figure A8. Mean factorial effects calculated from caspase 3/7 activity assay values for primary rat hepatocytes at two time points in the presence of six drugs. Error bars represent the standard error across five or more biological replicates, and * denotes statistical significance.

Primary rat hepatocytes
LDH release
Assay value

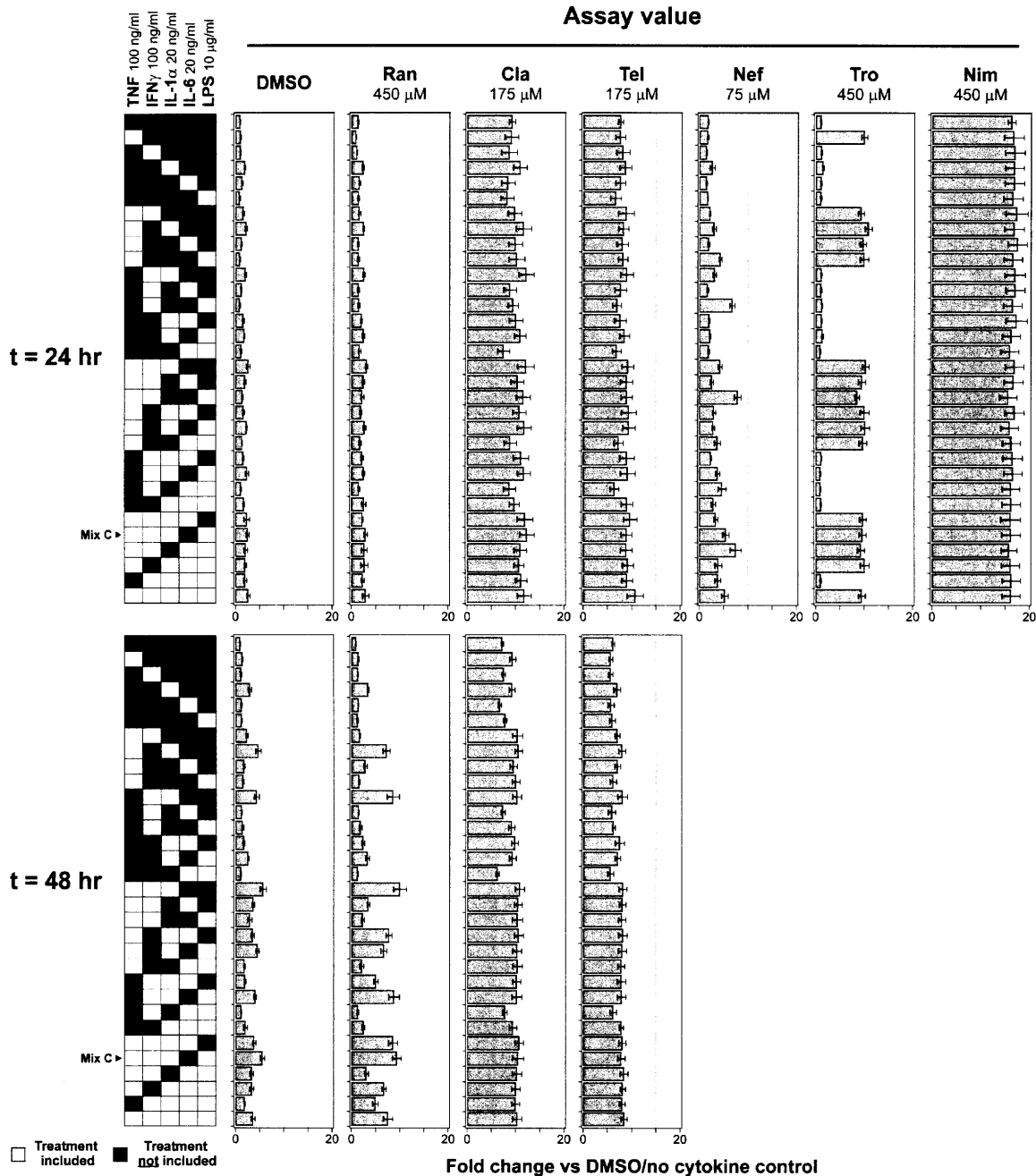


Figure A9. Mean LDH release assay values for primary rat hepatocytes at two time points in the presence of six drugs. Error bars represent the standard error across five or more biological replicates.

Primary rat hepatocytes
LDH release
Factorial effect

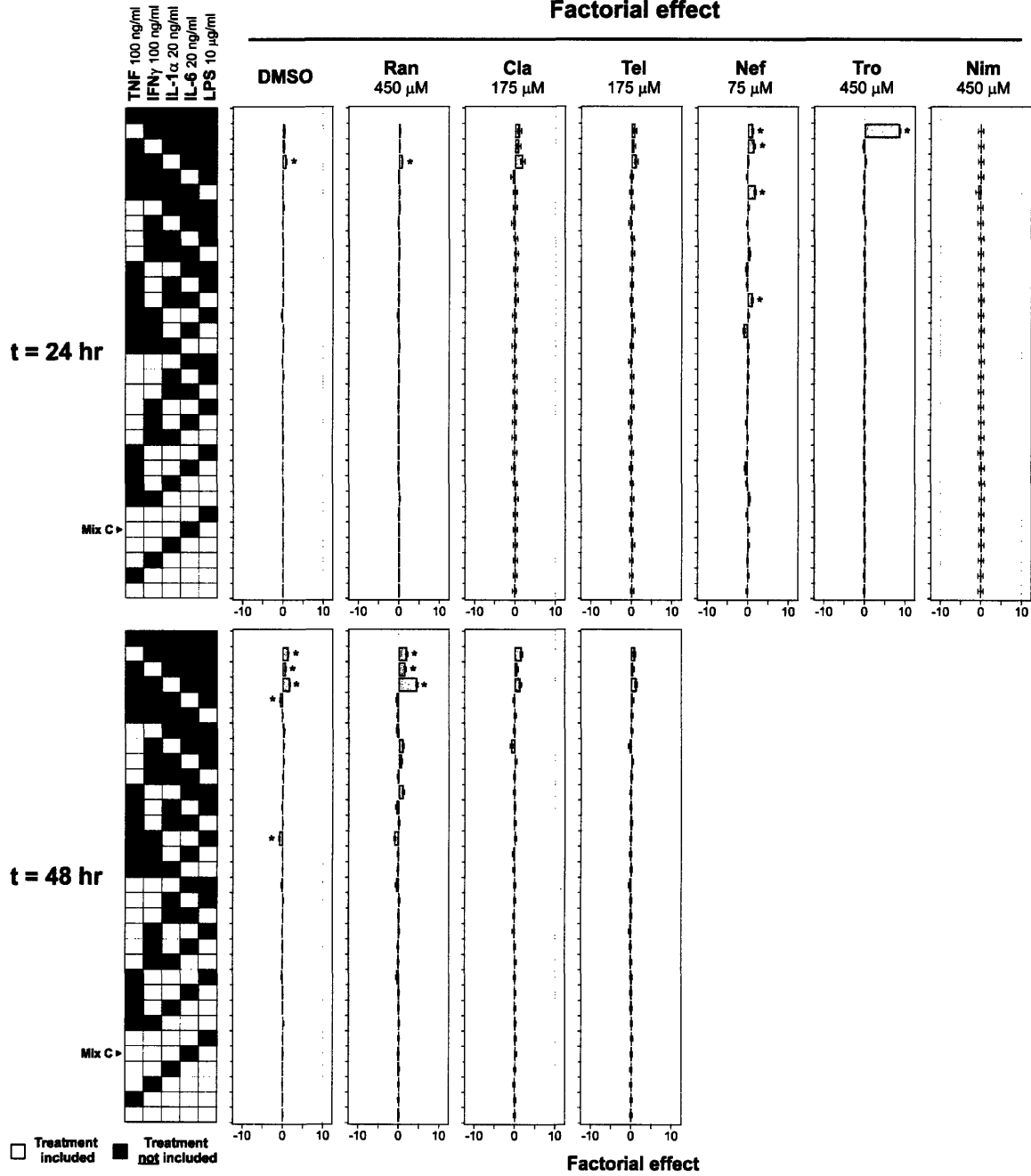


Figure A10. Mean factorial effects calculated from LDH release assay values for primary rat hepatocytes at two time points in the presence of six drugs. Error bars represent the standard error across five or more biological replicates, and * denotes statistical significance.